ORGANOMETALLICS

Article

pubs.acs.org/Organometallics

Reductive Elimination from Platinum(IV) Aminotroponiminate Dimethyl Complexes Promoted by Sterically Hindered Lewis Bases

Elise Traversa,[†] Joseph L. Templeton,*[,†] Hiu Yan Cheng,[‡] Megan Mohadjer Beromi,[‡] Peter S. White,[†] and Nathan M. West*[,‡]

[†]W.R. Kenan Laboratory, Department of Chemistry, University of North Carolina, Chapel Hill, North Carolina 27599-3290, United States

[‡]Department of Chemistry and Biochemistry, University of the Sciences, 600 South 43rd Street, Philadelphia, Pennsylvania 19063, United States

Supporting Information

ABSTRACT: A series of Pt^{II} and Pt^{IV} aminotroponimate (ATI = *N*-tolyl-aminotroponiminate) complexes has been prepared. The Pt^{II} complex (ATI)Pt(CH_3)(SMe_2) (**1a**) is synthesized from the reaction of [Li][ATI] with (Me)(Cl)Pt-(SMe_2)$_2$. Addition of either ethylene or carbon monoxide to **1a** results in the formation of (ATI)Pt(CH_3)(η^2-C_2H_4) (**1b**) or (ATI)Pt(CH_3)(CO) (**1c**), respectively. Oxidative addition of MeOTf or MeI to **1a** results in formation of the Pt^{IV} complex [(ATI)Pt(CH_3)$_2$(X)(SMe_2)] (X = OTf (**3**), I (**2**)). Complex **3** reacts with isocyanides, which replace the triflate ligand to form [(ATI)Pt(CH_3)$_2$(CNR)(SMe_2)][OTf] (**4**). Complex **3** also undergoes ligand substitution reactions with azide or cyanide to form (ATI)Pt(CH_3)$_2$(N_3)(SMe_2) (**5a**) or (ATI)Pt(CH_3)$_2$(CN)(SMe_2) (**5b**). Addition of PR_3 results in the substitution product [(ATI)Pt(CH_3)$_2$(PR_3)(SMe_2)][OTf] for phosphines with cone angles ≤136° ($P(OMe)_3$, PMe_3, PMe_2Ph). The Pt^{IV} complex [(ATI)Pt(CH_3)$_2$(PPh_2Me)(SMe_2)][OTf] (**6c**) reductively eliminates [PMe_2Ph_2][OTf] or [SMe_3][OTf] to form the Pt^{II} complex (ATI)Pt(CH_3)(PPh_2Me) (**7a**) in solution at room temperature. Addition of 1 equiv of PPh_3, which has a cone angle of 145°, results in the formation of 50% of Pt^{II}(ATI)Pt(CH_3)(PR_3) and [$MePPh_3$][OTf]. Reaction of **3** with PCy_3, which has a cone angle of 170°, yields complete and immediate conversion to (ATI)Pt(CH_3)(SMe_2) and [$MePCy_3$][OTf].

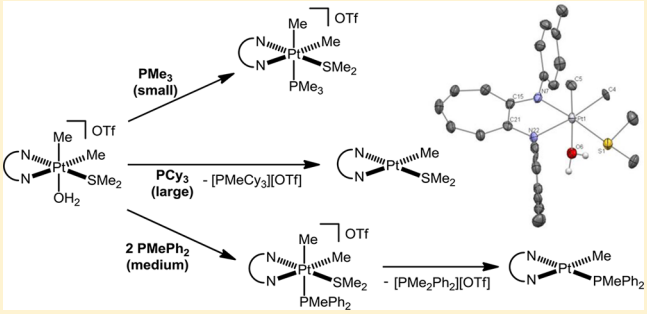

INTRODUCTION

Reductive elimination of C−X bonds is a critical step in the catalytic functionalization of small molecules using a d^8/d^6 transition-metal catalytic cycle.[1−4] These C−X eliminations have been known for Pt^{IV} since the discovery of the Shilov oxidation of methane to methanol[2,5] but have remained elusive until recently. There have been studies in the literature of C−N, C−O, C−I, C−C, and C−H bond forming reductive eliminations,[1,6−11] but there has been less work done on studying the formation of C−P and C−S bonds using late metals;[12−18] these reactions could be particularly useful for the catalytic synthesis of chiral phosphines. We report herein the reductive elimination of CH_3−P and CH_3−S bonds from Pt^{IV} aminotroponiminate (ATI) complexes at room temperature.

Goldberg and Templeton have shown that *β*-diiminate (nacnac) ligated Pt^{II} methyl complexes will activate the C−H bonds of alkanes and ethers with elimination of methane, forming Pt^{II} olefin hydride species.[19−23] We sought to extend this chemistry to the aminotroponiminate class of ligands, which are similarly symmetrical mononanionic bidentate nitrogen ligands that form a five-membered chelate rather than the six-membered chelate formed by the nacnac ligands. The ATI ligand is essentially an anionic analogue of a traditional *α*-diimine ligand.[24−29] The smaller ligand bite angle has been shown in the past to have a significant effect on the potential for oxidative addition and reductive elimination.[30−33] The aminotroponiminate ligands also eliminate one major problem with nacnac compounds, which is the nucleophilicity of the *γ*-carbon of the ligand, which has prevented the addition of electrophiles to the metal center in (nacnac)Pt^{II} complexes. Despite the large number of bidentate nitrogen ligands that have been put on Pt, no reports of (ATI)Pt complexes appear in the literature.

Neutral four-coordinate Pt^{II} ATI complexes readily undergo oxidative addition of methyl iodide and methyl triflate to form stable Pt^{IV} ATI complexes. The Pt^{IV} complexes formed by oxidative addition of methyl triflate contain a labile ligand which can be readily replaced by isocyanides, azides, cyanides, and phosphines. Cationic Pt^{IV} complexes of small phosphines are stable. However, bulky phosphines favor reductive elimination of R_3PMe^+; the presence of excess dimethyl sulfide in solution also leads to the elimination of Me_3S^+. Experiments using phosphines with various steric and electronic properties

Received: January 16, 2013
Published: March 5, 2013

have been used to probe the P−C reductive elimination reaction, and their results are reported below.

RESULTS AND DISCUSSION

Synthesis and Structure of (ATI)Pt(CH$_3$)(L) (1). The reaction between LiATI (ATI = *N*-tolyl-aminotroponiminate) and (Me)(Cl)Pt(SMe$_2$)$_2$ for 2 h yielded (ATI)Pt(CH$_3$)(SMe$_2$) (**1a**) and LiCl (eq 1). We have used the *p*-tolyl-substituted ATI

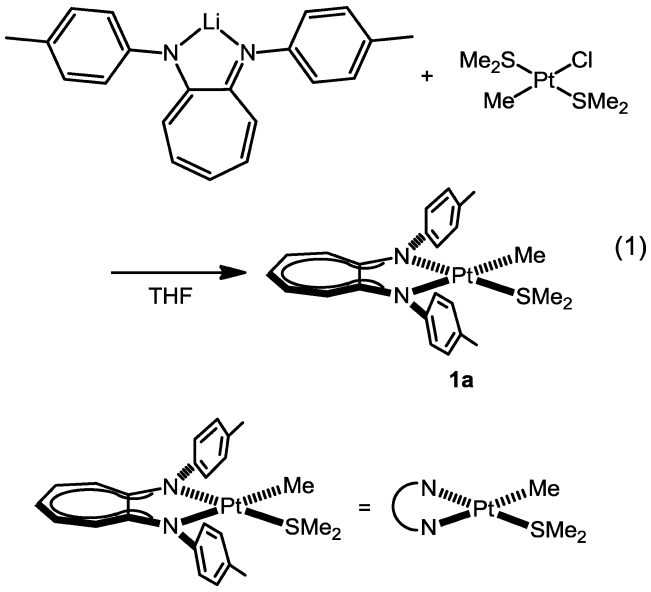

ligand so that the tolyl methyl groups provide us with an NMR handle on the complexes outside of the aromatic region. Complex **1a** is air stable and can be purified via column chromatography; it degrades over time at room temperature, and so the product was stored in a freezer. Brown crystals suitable for X-ray diffraction were obtained by layering a solution of **1a** in diethyl ether with pentane and cooling it to −35 °C (Figure 1). The bite angle of the ATI chelate is 77°, typical for a five-membered bidentate nitrogen ligand bound to platinum.[34,35] The ATI ligand tolyl rings are twisted nearly orthogonally to the plane containing the platinum chelate, while the flat 10-π-electron ATI backbone lies in the PtN$_2$SC plane. The Pt1−C1 and Pt1−S1 bond lengths of 2.08 and 2.25 Å, respectively, are also consistent with values observed in related structures, such as the Tp′Pt^{II}(Me)(SMe$_2$) complex, which contains a Pt−C bond length of 2.05 Å and Pt−S bond length of 2.25 Å.[36] The trans influence of the methyl group causes the Pt1−N4 bond (2.09 Å) to increase by 0.06 Å in comparison to the Pt1−N19 bond (2.03 Å), which is trans to the dimethyl sulfide.

A procedure to synthesize the monomethyl (nacnac)Pt^{II} ethylene and CO complexes has been reported.[21] We have synthesized (*N*-tolyl-ATI)Pt(CH$_3$)(L) (**1**: L= C$_2$H$_4$ (**1b**), CO (**1c**)) using an analogous procedure (eq 2). Stirring LiATI with (Me)(Cl)Pt(SMe$_2$)$_2$ for 15 min followed by addition of either ethylene or CO generates **1b**,**c** in modest yields. The ^{1}H NMR spectra of **1b**,**c** are similar, but the signals for the platinum-bound methyl groups are significantly shifted from one another. In the ^{1}H NMR spectrum of **1b**, the Pt−Me resonance appears at −0.27 ppm with $^2J_{Pt-H}$ = 71 Hz. The Pt−Me resonance of **1c** appears at 0.25 ppm with $^2J_{Pt-H}$ = 70 Hz. The bound ethylene in **1b** appears as a singlet at 2.89 ppm with platinum satellites ($^2J_{Pt-H}$ = 58 Hz) in the ^{1}H NMR spectrum and rotates freely on

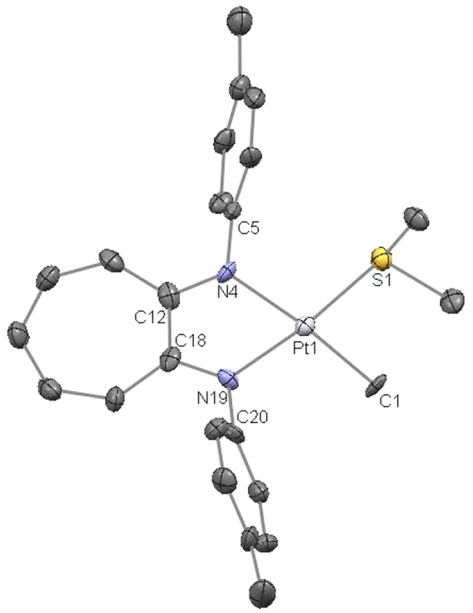

Figure 1. X-ray structure of (ATI)Pt(CH$_3$)(SMe$_2$) (**1a**). Thermal ellipsoids are drawn at the 50% probability level. The hydrogen atoms are omitted for clarity. Selected bond distances (Å) and angles (deg): Pt(1)−N(19) = 2.029(7); Pt(1)−C(1) = 2.077(7); Pt(1)−N(4) = 2.092(7); Pt(1)−S(1) = 2.249(2); N(19)−Pt(1)−N(4) = 77.2(3).

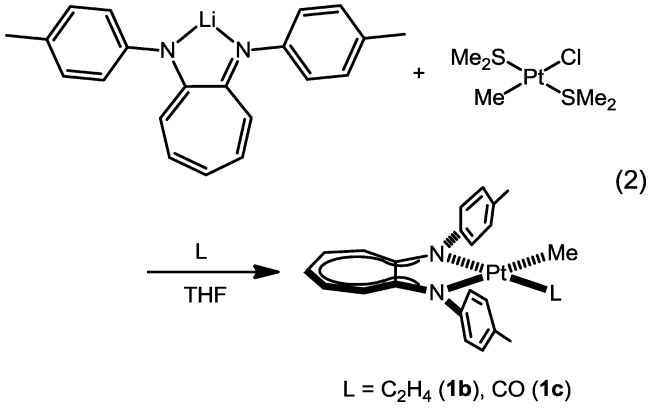

the NMR time scale at temperatures well below 300 K. The coalescence temperature of the ethylene signals in the ^{1}H NMR spectrum was found to be 228 K, suggesting a rotational barrier of less than 12 kcal/mol. This stands in contrast to the nacnac analogue, (nacnac)Pt(CH$_3$)(C$_2$H$_4$), which is static at room temperature and has a barrier to rotation of 16.7 kcal/mol;[21] this illustrates the fact that the ligands are less sterically encumbered by the ATI aryl rings than in the nacnac complexes. In (nacnac)Pt(CH$_3$)(C$_2$H$_4$) the methyl carbon to aryl ipso carbon distance is 2.9 Å, whereas in **1b** the C1−C20 distance is 3.2 Å.

If HATI is stirred with Me$_4$Pt$_2$(μ-SMe$_2$)$_2$ overnight in CH$_2$Cl$_2$/pentane, the major product is **1a**. A small amount of (ATI)Pt(H)(1-pentene) can be observed by ^{1}H NMR; however, the yield of this product is much lower than in the analogous reaction with Hnacnac.[21] We postulate that the reason for this is that the reduced steric inhibition of the ATI ligand allows the SMe$_2$ ligand to coordinate more easily than in the nacnac case and SMe$_2$ coordination prevents C−H activation.

dx.doi.org/10.1021/om400034y | *Organometallics* 2013, 32, 1938−1950

Oxidative Addition of MeI and MeOTf to (ATI)Pt(CH_3)-(SMe_2). Addition of 1.2 equiv of MeI to **1a** in CH_2Cl_2 yields the oxidative addition product (ATI)Pt(CH_3)$_2$(I)(SMe_2) (**2**) (eq 3). Oxidative addition of primary alkyl halides to square-

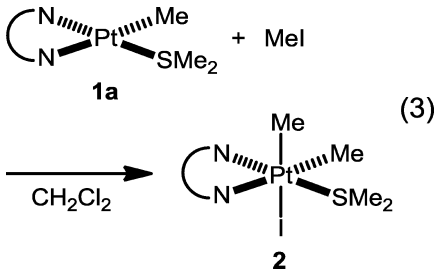

(3)

planar complexes usually occurs in a trans fashion via an S_N2 reaction, though some isomerization is known to occur.[37] Although four NMR distinct isomers are possible, only one is observed by NMR spectroscopy (Figure 2). The ^{1}H NMR spectrum shows resonances at 1.51 ppm for the Pt−Me trans to nitrogen ($^2J_{Pt-H}$ = 71 Hz) and at 0.71 ppm for the Pt−Me trans to iodide ($^2J_{Pt-H}$ = 64 Hz). The assignment is based on data for Pt^{IV} complexes of the form (LL)Pt(Me)$_3$X.[38−40] Since the coordinated sulfur in the dimethyl sulfide ligand is pyramidal, the Pt−SMe_2 methyl groups are diastereotopic and appear at 2.34 ppm ($^3J_{Pt-H}$ = 32 Hz) and 1.79 ppm ($^3J_{Pt-H}$ = 35 Hz) in the Pt^{IV} product. Compound **2** is stable at room temperature and can be purified via column chromatography.

The addition of 1.2 equiv of MeOTf to a −78 °C solution of **1a** in CH_2Cl_2 yields complex **3**, which can be purified by column chromatography (Scheme 1). The ^{1}H NMR spectrum of this complex is unusual: a broad singlet with platinum satellites which integrates for 6H appears at 1.05 ppm ($^2J_{Pt-H}$ = 71 Hz), and another broad singlet with platinum satellites integrating for 6H appears at 1.98 ppm ($^3J_{Pt-H}$ = 32 Hz) (Figure 3). The ^{13}C NMR spectrum displays a broad signal at 3.1 ppm ($^1J_{Pt-C}$ = 619 Hz) with platinum satellites. The platinum coupling of 71 Hz to the proton signal at 1.05 ppm in the ^{1}H NMR spectrum and its integration for 6H, combined with the broad signal with platinum satellites at 3.1 ppm in the ^{13}C NMR spectrum, are suggestive of two methyl groups bound to platinum which are fluxional on the NMR time scale. Upon cooling, the ^{1}H signal near 1 ppm in the ^{1}H NMR spectrum broadens, disappears into the baseline, and then reappears at low temperature as four distinct methyl signals, indicating the presence of two NMR distinct complexes. Two methyl signals are seen via low-temperature ^{1}H NMR spectroscopy for each compound (one axial and one equatorial with respect to the ATI plane) (Figure 3). The ratio of the two complexes varies with each trial.

Scheme 1. Formation and Equilibrium of Complexes 3a,b

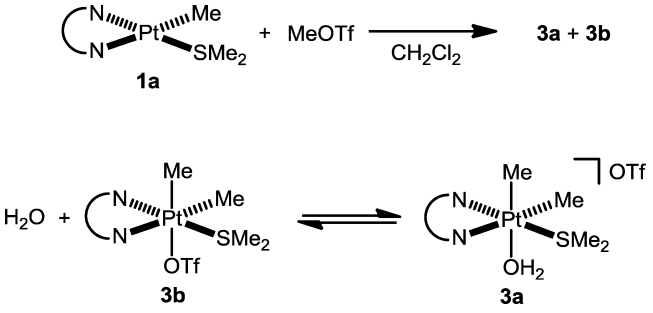

Puddephatt et al. noticed similar spectroscopic behavior following the oxidative addition of MeOTf to Pt^{II} dimethyl complexes containing various bidentate nitrogen ligands.[41,42] The Pt^{IV} complexes prepared by Puddephatt et al. reductively eliminate ethane at room temperature;[41] however, low-temperature NMR studies indicate that the complex is an equilibrium mixture of two complexes. They propose that the two complexes are a neutral triflato complex and a cationic aquo complex which are in equilibrium with each other. Replacement of the triflate ligand by adventitious water is a facile process due to the lability of the triflate anion. The ratio of the two complexes is highly variable, since formation of the aquo complex is dependent upon adventitious water in solution (Scheme 1). Similar behavior has been observed for diphosphine-ligated trimethyl Pt^{IV} species.[41,43]

The Pt−OH_2 resonance in **3a** can be observed at 5.5 ppm via low-temperature ^{1}H NMR spectroscopy. This low-temperature probe is the only viable NMR technique that distinguishes **3a** from **3b**. One other Pt−OH_2 species has been characterized via low-temperature NMR spectroscopy, and it is a Pt^{II} complex with a coordinated water resonance at 6.51 ppm.[44] Reactions performed with mixtures of **3a** and **3b** (referred to as **3** from here on) are conducted with **3a** and **3b** generated in situ and kept air-free; the ratio of **3a** to **3b** appears to have no effect on the reactivity we observe.

Slow evaporation of a methylene chloride solution of **3a,b** at room temperature produced X-ray-quality crystals of [(ATI)-Pt(CH_3)$_2$(OH_2)(SMe_2)][OTf] (**3a**) (Figure 4). The solid-state structure of **3a** is a distorted octahedron around the Pt^{IV} center, and the geometry of the ATI ligand is similar to that seen for compound **1a**, with a bite angle of 77°. The Pt1−S1 bond distance of 2.32 Å is slightly longer than in **1a** (2.25 Å). The equatorial Pt1−C4 bond length is longer than the axial Pt1−C5 bond length, 2.08 vs 2.04 Å, respectively, due to the weaker water ligand being trans to C5. The Pt1−O6 bond length of 2.26 Å is similar to the bond length in the aquo complex synthesized by Puddephatt et al. (2.28 Å).[41] This long Pt−O

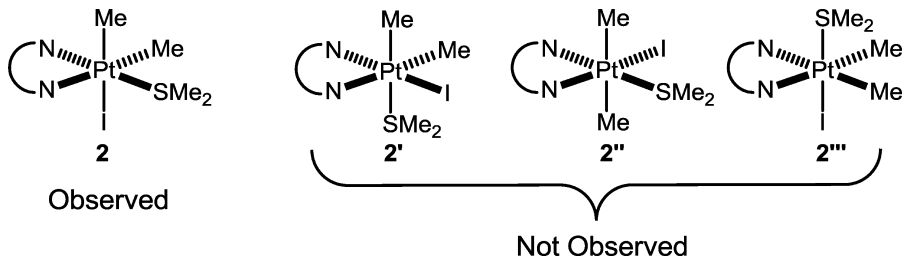

Figure 2. Four isomers possible from the oxidative addition of MeI to **1a** yielding **2**.

dx.doi.org/10.1021/om400034y | *Organometallics* 2013, 32, 1938−1950

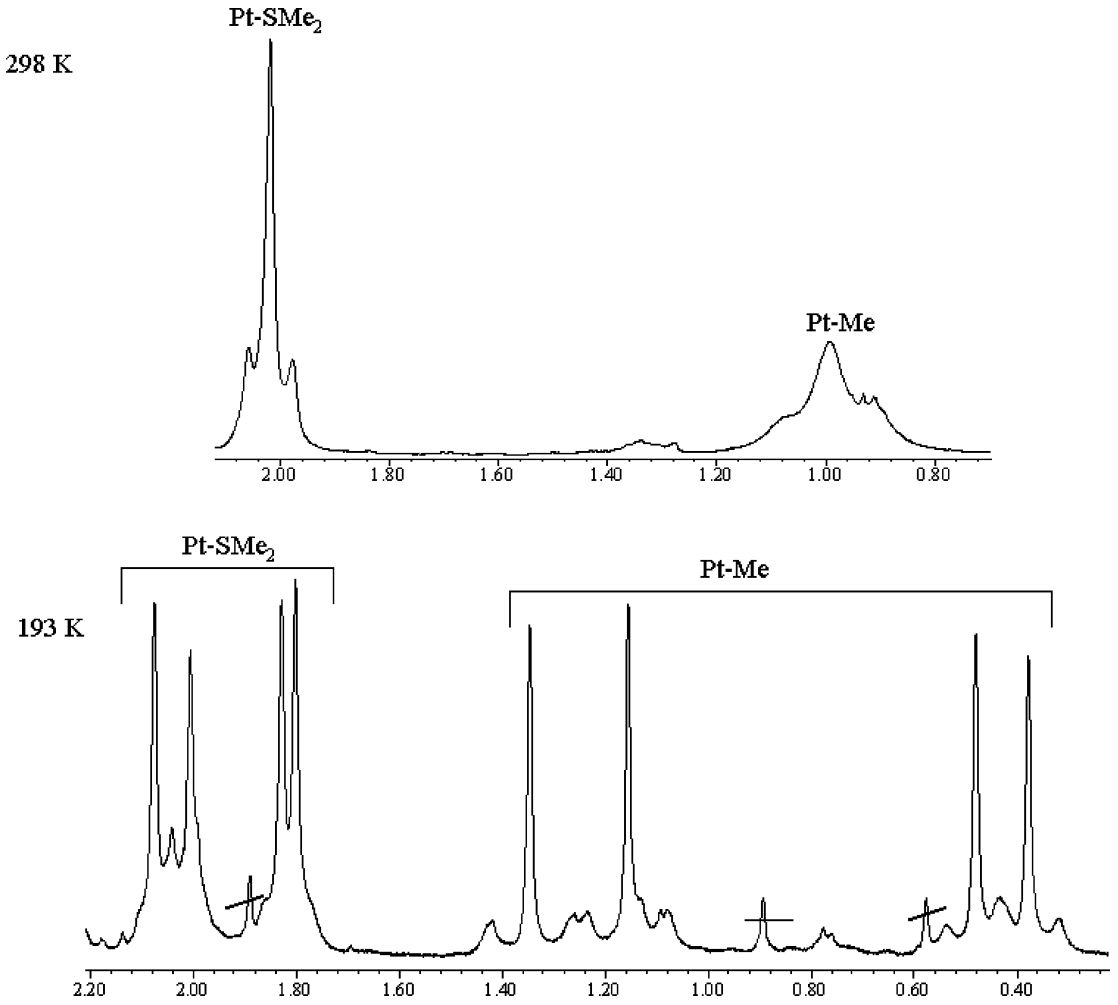

Figure 3. ^{1}H NMR of the Pt−Me and Pt−SMe_2 groups of **3a**,**b** at 298 K (top) and 193 K (bottom).

bond distance is consistent with the labile nature of the water ligand.

Substitution of Aquo or Triflate Ligands. The aquo/triflate ligand on **3** is labile, which opens routes to the synthesis of other Pt^{IV} complexes. Addition of an excess of RNC to a solution of **3** in CH_2Cl_2 produces a solution of $[(ATI)Pt(CH_3)_2(RNC)(SMe_2)][OTf]$ (**4a**,**b**) (eq 4). This is a facile

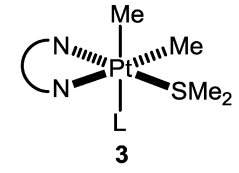

3

L = OTf (**3a**), H_2O (**3b**)

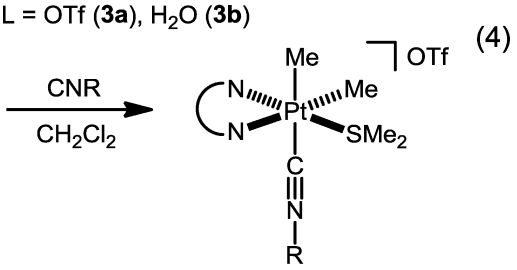

(4)

R = *t*Bu (**4a**), 2,6-$(CH_3)_2C_6H_3$ (**4b**)

substitution reaction, with formation of the product within minutes. The compound is air stable and can be purified via column chromatography. The ^{1}H NMR spectrum is sharp in comparison to **3**; the Pt methyl groups appear at 1.18 ppm ($^2J_{Pt-H}$ = 62 Hz) and 0.46 ppm ($^2J_{Pt-H}$ = 62 Hz), and the dimethyl sulfide methyl groups appear at 2.22 ppm ($^3J_{Pt-H}$ = 34 Hz) and 2.09 ppm ($^3J_{Pt-H}$ = 37 Hz). The sharpness of the spectrum shows that, unlike **3**, the complex is not fluxional on the NMR time scale. A C≡N absorbance can be detected by IR spectroscopy at 2217 cm^{-1} for the *tert*-butyl isocyanide adduct **4a** and at 2196 cm^{-1} for the aryl isocyanide **4b**; these C≡N stretches are at much higher frequency than those for the free isocyanides, which indicates that the Pt is electron deficient and unable to back-bond to the isocyanides so that they act as σ-donating-only ligands (Table 1). The stretching frequency of **4a** is 25 cm^{-1} higher than that for the neutral Pt^{IV} species (nacnac)$PtMe_3$(CN*t*Bu), further illustrating the high electrophilicity of **4a**.[45]

Slow evaporation of a methylene chloride solution of **4a** at room temperature produced X-ray-quality crystals (Figure 5). The only noteworthy difference in the solid-state structure of **4a** versus that of **3a** is that the axial Pt methyl carbon bond has slightly lengthened, 2.07 Å in **4a** and 2.04 Å in **3a**, due to the greater trans influence of the isonitrile ligand vs that of the aquo ligand; the axial Pt−CH_3 bond and the Pt−CNR bond are equal at 2.08 Å.

dx.doi.org/10.1021/om400034y | *Organometallics* 2013, 32, 1938−1950

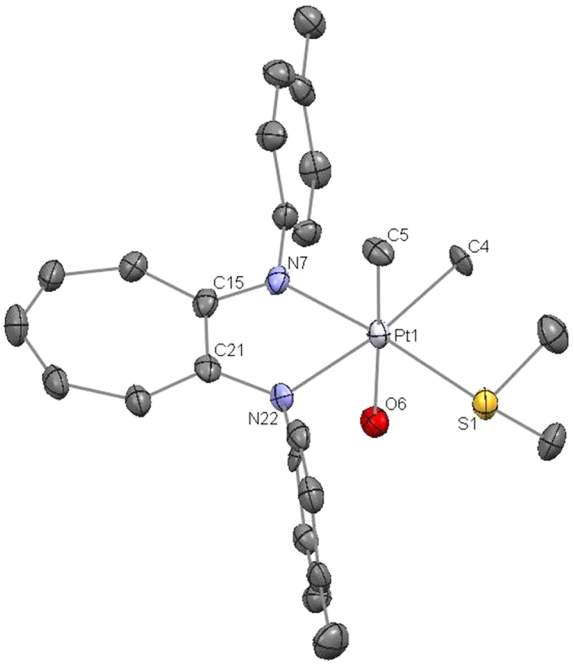

Figure 4. X-ray structure of [(ATI)Pt(CH_3)$_2$(OH_2)(SMe_2)][OTf] (**3a**). Thermal ellipsoids are drawn at the 50% probability level. The hydrogen atoms and the triflate counterion are removed for clarity. One hydrogen atom on O(6) was found, and one was calculated. Selected bond distances (Å) and angles (deg): Pt(1)−O(6) = 2.263(5); Pt(1)−C(5) = 2.037(7); Pt(1)−N(7) = 2.039(6); Pt(1)−C(4) = 2.077(7); Pt(1)−N(22) = 2.119(6); Pt(1)−S(1) = 2.3197(19); N(7)−Pt(1)−N(22) = 77.0(2).

Table 1. C≡N Stretching Data for 4 and Free Isocyanides

compd	C≡N stretch (cm^{-1})
R = tBu (**4a**)	2217
R = 2,6-dimethylphenyl (**4b**)	2196
tert-butyl isocyanide	2136
2,6-dimethylphenyl isocyanide	2116
(nacnac)$PtMe_3$(CNtBu)[45]	2192

Addition of organic azides, such as phenyl azide, to **3** did not result in any observed reaction; however, substitution of the aquo/triflate ligand with NaN_3 was successful. Vigorous stirring of **3** in a solution of CH_2Cl_2 with a large excess of NaN_3 overnight yields the substitution product (ATI)Pt(CH_3)$_2$(N_3)(SMe_2) (**5a**) (eq 5). The ^{1}H spectrum of **5a** is similar to that of

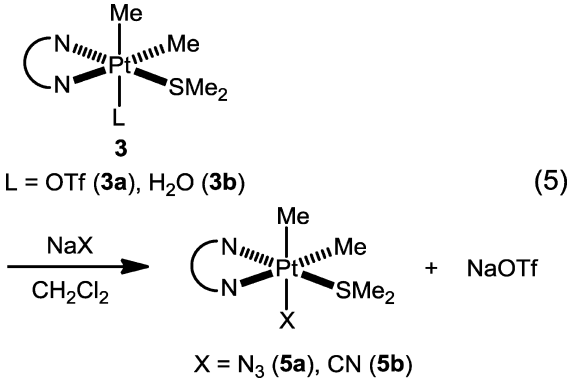

4a,b with the Pt−Me signal trans to the ATI nitrogen (0.38 ppm) and the Pt−Me signal trans to N_3 (1.07 ppm) shifted 0.6 ppm from one another; two distinct signals for the diastereotopic Pt−SMe_2 methyl groups appear around 2 ppm. The reaction can be monitored via IR spectroscopy, as **5a** shows an IR stretch of ν_{N_3} 2038 cm^{-1} for the linear azide entity.

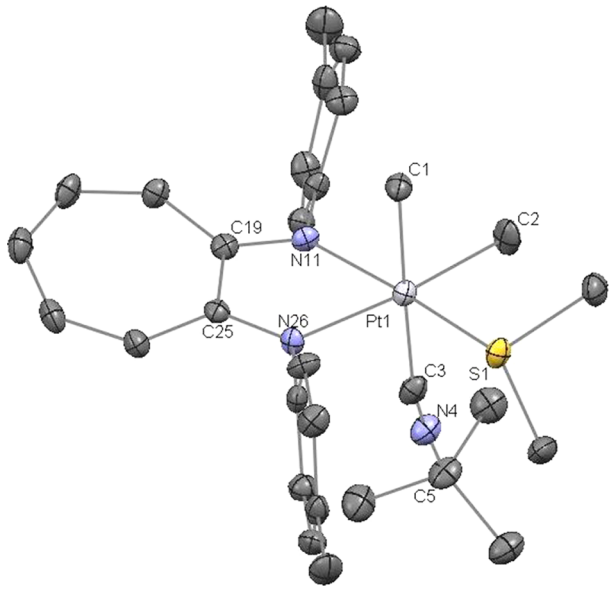

Figure 5. X-ray structure of [(ATI)Pt(CH_3)$_2$(^{t}BuNC)(SMe_2)][OTf] (**4a**). Thermal ellipsoids are drawn at the 50% probability level. The hydrogen atoms and the triflate counterion are removed for clarity. Selected bond distances (Å) and angles (deg): Pt(1)−N(1) = 2.048(3); Pt(1)−C(1) = 2.071(3); Pt(1)−C(3) = 2.082(3); Pt(1)−C(2) = 2.083(3); Pt(1)−N(26) = 2.115(2); Pt(1)−S(1) = 2.317(8); C(3)−N(4) = 1.142(4); N(11)−Pt(1)−N(26) = 76.85(10).

Using the same methods as with NaN_3, (ATI)Pt(CH_3)$_2$(CN)(SMe_2) (**5b**) was synthesized via a reaction with NaCN. The reaction can also be monitored via IR spectroscopy, as **5b** shows an IR stretch for the cyanide of $\nu_{C\equiv N}$ 2301 cm^{-1}; this stretch is higher in energy in comparison to the value of 2125 cm^{-1} reported for (bpy)$PtMe_3$(CN).[46] The ^{1}H NMR spectra of **5a** and **5b** are similar, but the downfield Pt−-Me shifts from 1.07 ppm ($^2J_{Pt-H}$ = 70 Hz) for **5a** to 0.69 ppm ($^2J_{Pt-H}$ = 56 Hz) in **5b**; this upfield shift and reduction in coupling constant is consistent with known (L)$_2$$PtMe_3$(CN) complexes.[46,47]

Addition of Phosphines to 3. Addition of 1 equiv of PMe_3 to a solution of **3** in CH_2Cl_2 at room temperature produces the expected aquo/triflate displacement product [(ATI)Pt(CH_3)$_2$(PMe_3)(SMe_2)][OTf] (**6a**) (eq 6). The ^{1}H NMR spectrum of this product clearly shows two Pt−Me signals which are coupled to phosphorus with $^3J_{P-H}$ = 9 Hz for the downfield methyl protons and $^3J_{P-H}$ = 8 Hz for the upfield methyl protons. Only one of the two diastereotopic Pt−SMe_2 methyl signals is visible. It appears at 2.23 ppm and is quite broad. The other Pt−SMe_2 methyl signal is obscured by the bound PMe_3 signal. The ^{31}P NMR spectrum also confirms the addition of PMe_3 to the platinum center by exhibiting a singlet at −30.0 ppm having platinum satellites with $^1J_{Pt-P}$ = 1101 Hz. The compound can be purified by column chromatography and is also stable in solution for several days at room temperature in air. The stability indicates that the PMe_3 is bound tightly to the Pt, as it would rapidly oxidize to $OPMe_3$ under these conditions if the binding was reversible; this oxidation due to reversible

dx.doi.org/10.1021/om400034y | *Organometallics* 2013, 32, 1938−1950

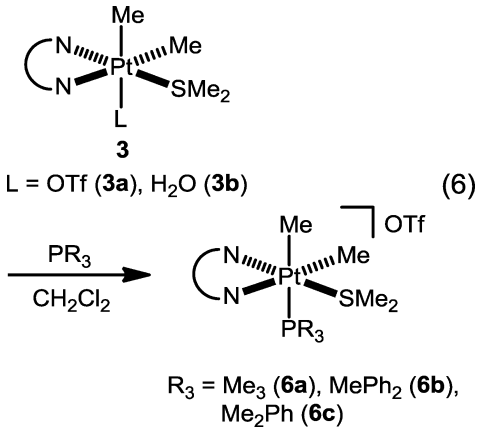

coordination does occur in the related complex (nacnac)Pt-$(H)_2(SiPh_3)(PMe_3)$.[48]

A solution of **6a** in methylene chloride was layered with hexanes and stored at −35 °C. This recrystallization produced brown crystals suitable for X-ray diffraction (Figure 6). The

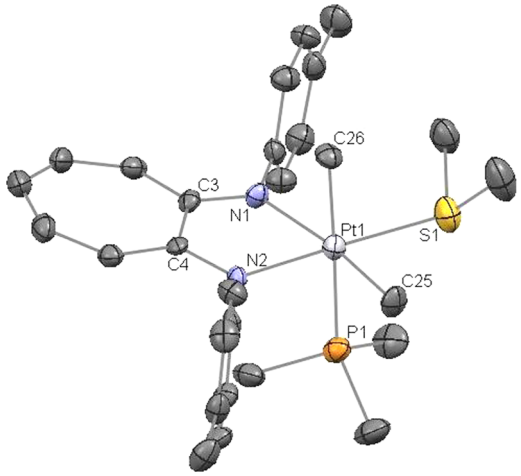

Figure 6. X-ray structure of $[(ATI)Pt(CH_3)_2(PMe_3)(SMe_2)][OTf]$ (**6a**). Thermal ellipsoids are drawn with 50% probability. The hydrogen atoms, triflate counterion, and a molecule of water are removed for clarity. Selected bond distances (Å) and angles (deg): Pt(1)−N(2) = 2.071(3); Pt(1)−C(26) = 2.108(4); Pt(1)−S(1) = 2.3322(10); Pt(1)−C(25) = 2.092(4); Pt(1)−N(1) = 2.159(3); Pt(1)−P(1) = 2.4176(10); N(2)−Pt(1)−N(1) = 75.64(13).

solid-state structure of **6a** confirms replacement of the aquo/triflate ligand on **3** with PMe_3. The bond length of 2.11 Å for the Pt1−C26 trans to PMe_3 is longer than that for either the isocyanide adduct **4a** (2.07 Å) or the aquo adduct **3a** (2.04 Å), which is in accordance with the increasing trans influence from H_2O to RNC to PMe_3.[49,50] The Pt1−S1 bond length of **6a** is also similar to that of **3a** and **4a** (2.32 Å) at 2.33 Å. Although the diastereotopic SMe_2 signals in the ^1H NMR show significant line broadening, low-temperature ^1H NMR studies show that the signals for the diastereotopic SMe_2 methyl protons sharpen upon cooling.

Due to successful displacement of the triflate/aquo ligand in **3** with PMe_3, which has a cone angle of 118°, more sterically demanding phosphorus containing ligands were investigated (Table 2).[51] The addition of 1 equiv of $PPhMe_2$, which has a cone angle of 122°, to **3** at room temperature yields the phosphine adduct $[(ATI)Pt(CH_3)_2(PPhMe_2)(SMe_2)][OTf]$

Table 2. Pt−P Coupling Data for Complexes 6a−d

PR_3 (**6**)	$^1J_{Pt-P}$ (Hz)	cone angle (deg)[51]
PMe_3 (**6a**)	1101	118
PMe_2Ph (**6b**)	1004	122
$PMePh_2$ (**6c**)	877	136
$P(OMe)_3$ (**6d**)	1963	107

(**6b**). This complex can be purified by column chromatography and is stable in solution at room temperature for several days. The ^1H NMR spectra of **6a** and **6b** are quite similar, and the ^{31}P NMR spectrum of **6b** exhibits a signal at −24.1 ppm with platinum satellites: $^1J_{Pt-P}$ = 1004 Hz. The addition of 1 equiv of PPh_2Me, which has a cone angle of 136°, to **3** at room temperature results in the formation of $[(ATI)Pt(CH_3)_2(PPh_2Me)(SMe_2)][OTf]$ (**6c**). However, unlike **6a** and **6b**, **6c** is not stable over time in solution, and over 4 days at room temperature in solution, **6c** converts to a second product, **7a**. Complex **6c** is stable enough to be dried in vacuo and triturated with hexane to remove any excess $PMePh_2$ that may be present. The NMR of **6c** is analogous to that of **6a** and **6b**; the phosphorus signal appears at −23.8 ppm and has a Pt−P coupling constant of 877 Hz. It is interesting to note that, for the Pt^{IV} PR_3 complexes, the $^1J_{Pt-P}$ value decreases with increasing cone angle (Table 2). This is most likely indicative of weaker Pt−P bonds due to steric repulsion between PR_3 and the other ligands around Pt.

Complex **7a** exhibits a Pt−Me signal coupled to phosphorus with platinum satellites visible in the ^1H NMR spectrum at −0.34 ppm. The PPh_2Me methyl protons resonate as a doublet at 0.87 ppm. The ^{31}P NMR spectrum shows a peak at 1.5 ppm with $^1J_{Pt-P}$ = 3979 Hz. The ^1H and ^{13}C NMR spectra show resonances corresponding to only one Pt−Me group and bound PPh_2Me. The NMR data are consistent with the Pt^{II} species $(ATI)Pt(CH_3)(PPh_2Me)$ (**7a**), and this was confirmed by X-ray crystallography.

Slow evaporation of a solution of **7a** in methylene chloride produced clear yellow platelike crystals suitable for X-ray diffraction (Figure 7). The structure is similar to that of **1a**, with a distorted-square-planar geometry about the platinum center. The Pt(1)−P(1) bond length of 2.22 Å is significantly shorter than that in **6a** (2.42 Å); this also reflects the $^1J_{Pt-P}$ values of 3979 Hz for **7a** and 1101 Hz for **6a**.

In addition to the formation of the product **7c**, formation of $[PMe_2Ph_2][OTf]$ is observed by ^1H and ^{31}P NMR. We also observe the re-formation of broad methyl signals indicative of **3** in the ^1H NMR spectrum; as conversion increases and the concentration of free SMe_2 increases, the methyl signals shift slightly and become more broad, consistent with reversible SMe_2 binding to **3** (Figure 8). A signal at 3.00 ppm in the ^1H NMR for $[SMe_3][OTf]$ grows in increasingly as the concentration of SMe_2 goes up and that of **6c** goes down; the identity of this compound was confirmed by spiking a reaction mixture with independently synthesized $[SMe_3][OTf]$. The decomposition of **6c** yields about $^1/_2$ equiv of **7a** and $^1/_2$ equiv of **3**. No formation of $(ATI)Pt(Me)(SMe_2)$ (**1a**) is observed at any time; this is expected, because **1a** will react rapidly with $PMePh_2$ to form **7a**. If the reaction is conducted with 2 equiv or more of phosphine, then no $[SMe_3][OTf]$ is observed; only $[PMe_2Ph_2][OTf]$ is found and complete conversion to **7a** occurs (Scheme 2).

Addition of PPh_3, which has a cone angle of 145°, to a solution of **3** in CH_2Cl_2 at room temperature does not generate

dx.doi.org/10.1021/om400034y | Organometallics 2013, 32, 1938−1950

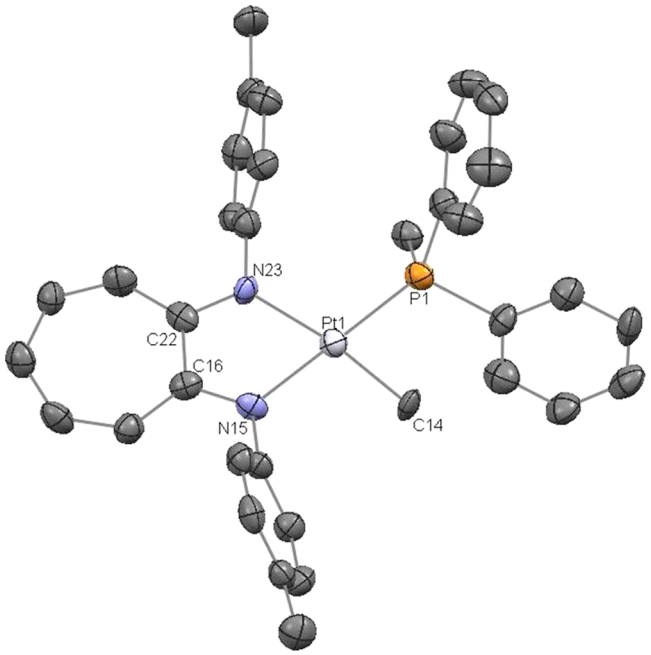

Figure 7. X-ray structure of (ATI)Pt(CH_3)(PPh_2Me) (**7a**). Thermal ellipsoids are drawn at the 50% probability level. The hydrogen atoms are removed for clarity. Selected bond distances (Å) and angles (deg): Pt(1)−N(23) = 2.090(6); Pt(1)−C(14) = 2.069(7); Pt(1)−N(15) = 2.074(7); Pt(1)−P(1) = 2.216(2); N(15)−Pt(1)−N(23) = 77.3(3).

an observable Pt^{IV} compound, but over the period of a few hours conversion of **3** to (ATI)Pt(CH_3)(PPh_3) (**7b**) is observed (eq 7). The ^{31}P NMR spectrum of **7b** has a single

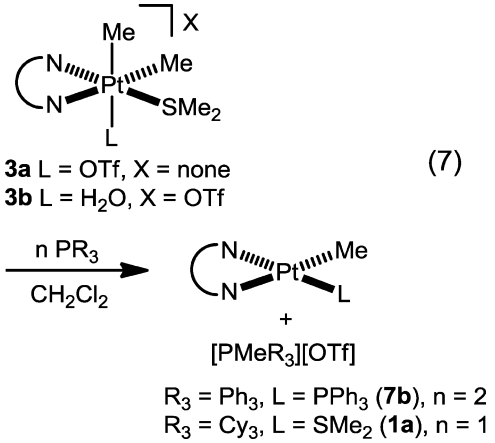

(7)

peak at 18.8 ppm with platinum satellites and $^1J_{Pt-P}$ = 4134 Hz, confirming addition of PPh_3 to the platinum center. The reaction can be monitored via ^1H and ^{31}P NMR spectroscopy, but the only Pt compounds observed are **3** and **7b**. Along with formation of **7b**, formation of [$PMePh_3$][OTf] is observed both by ^1H and ^{31}P NMR; no formation of [SMe_3][OTf] is observed. Two equivalents of PPh_3 is required for complete conversion of **3** to **7b**; addition of 1 equiv results in formation of $^1/_2$ equiv each of **7b** and the phosphonium salt and half of **3** remains. These data are consistent with a mechanism involving nucleophilic attack of the phosphine on one of the methyl groups in **3** (likely preceded by dissociation of OTf/H_2O) to re-form **1a**; **1a** will then readily react with another molecule of PPh_3 and form **7b** (Scheme 3). Direct synthesis of **7b** by the reaction of **1a** and PPh_3 confirms that ligand exchange is much faster than conversion of **3** to **7b**. If the reaction was going through a Pt^{IV} phosphine intermediate, which would be consistent with **6c** converting to **7a**, its formation would have to be rate limiting with reductive elimination or phosphine loss occurring rapidly; we cannot rule out this pathway, but it seems unlikely on the basis of the stability of **6c**.

In order to test whether the divergent reactivity observed with phosphine ligands was due to steric or electronic factors, we investigated the reactivity of PCy_3, which is electronically similar to PMe_3 but has a large cone angle of 170°. When 1 equiv of PCy_3 was added to **3** in CD_2Cl_2 at room temperature, we observed rapid and complete conversion to (ATI)Pt(CH_3)(SMe_2) (**1a**) and [$PMeCy_3$][OTf]; no Pt^{IV} phosphine complex could be observed. This reaction pathway is analogous to the reaction with PPh_3, but reductive elimination occurs at a faster rate, which prevents displacement of SMe_2 by PCy_3 in **1a**. These data are consistent with a mechanism that is dominated by steric factors; the increased rate of reaction is consistent with the greater nucleophilicity of PCy_3 versus PPh_3.

We also investigated the opposite end of the spectrum by using $P(OMe)_3$, which has a small cone angle of 107° but is less basic and more π acidic than PPh_3. The reaction of **3** and 1 equiv of $P(OMe)_3$ at room temperature forms the stable Pt^{IV} compound [(ATI)Pt(CH_3)$_2$($P(OMe)_3$)(SMe_2)][OTf] (**6d**), from which reductive elimination is not observed. This reaction is similar to the reaction with PMe_3, further indicating that the reductive elimination is dependent on the cone angle of the phosphine and not the electronic differences.

The strong correlation between ligand cone angle and either binding or nucleophilic attack on the Pt^{IV} methyl group explains why we do not observe attack on the methyl with N_3^- and CN^-, both of which are much better nucleophiles than PPh_3 (Scheme 4). On the basis of our observations, the Pt^{IV} metal center is the most electrophilic position on **3**, but if the steric bulk of the incoming nucleophile prevents it from forming a stable complex, the nucleophile will attack the electrophilic methyl group trans to the vacant site on Pt. Under such a mechanism, increasing the nucleophilicity of the incoming ligand will only increase the rate of C−X bond formation if the nucleophile has sufficient steric bulk. The mechanism of C−X bond formation from Pt^{IV} in systems such as the Shilov oxidation of methane to methanol has been shown to proceed through a similar nucleophilic attack mechanism of reductive elimination. A similar balance of binding to Pt^{IV} or attacking the Pt^{IV} methyl group is present in these reactions, and a sterically encumbering ligand system on the Pt catalyst may be able to increase the rate and selectivity of reductive elimination.

■ CONCLUSION

The platinum(II) aminotropimate complexes readily undergo oxidative addition with electrophilic methyl sources to yield dimethyl Pt(IV) complexes. The dimethyl Pt(IV) complexes will readily exchange their X ligand for a number of monodentate anionic or neutral ligands. In most cases this allows for the isolation of stable neutral or cationic dimethyl Pt(IV) complexes, but when bulky phosphine ligands are used, reductive elimination to form methyl Pt(II) species occurs. No reductive elimination of ethane is observed under any conditions, but methyl phosphonium species are reductively eliminated when bulky phosphine ligands are present. Whether or not reductive elimination occurs and the pathway by which it occurs are sensitive to the cone angle of the phosphine that is

dx.doi.org/10.1021/om400034y | Organometallics 2013, 32, 1938−1950

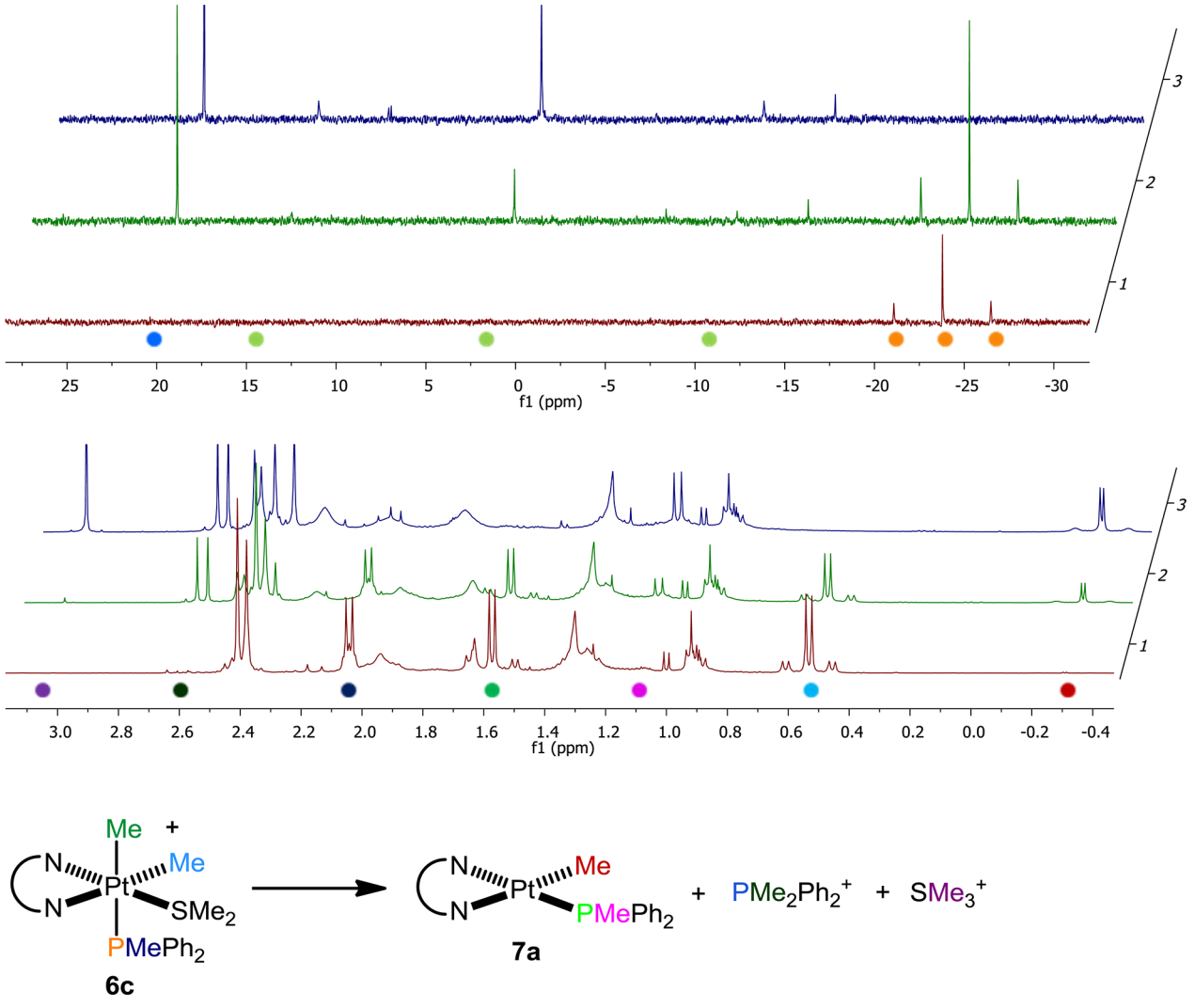

Figure 8. ^{31}P and ^{1}H NMR spectra showing the conversion of **6c** to **7a**.

Scheme 2. Proposed Mechanism for the Conversion of 6c to 7a

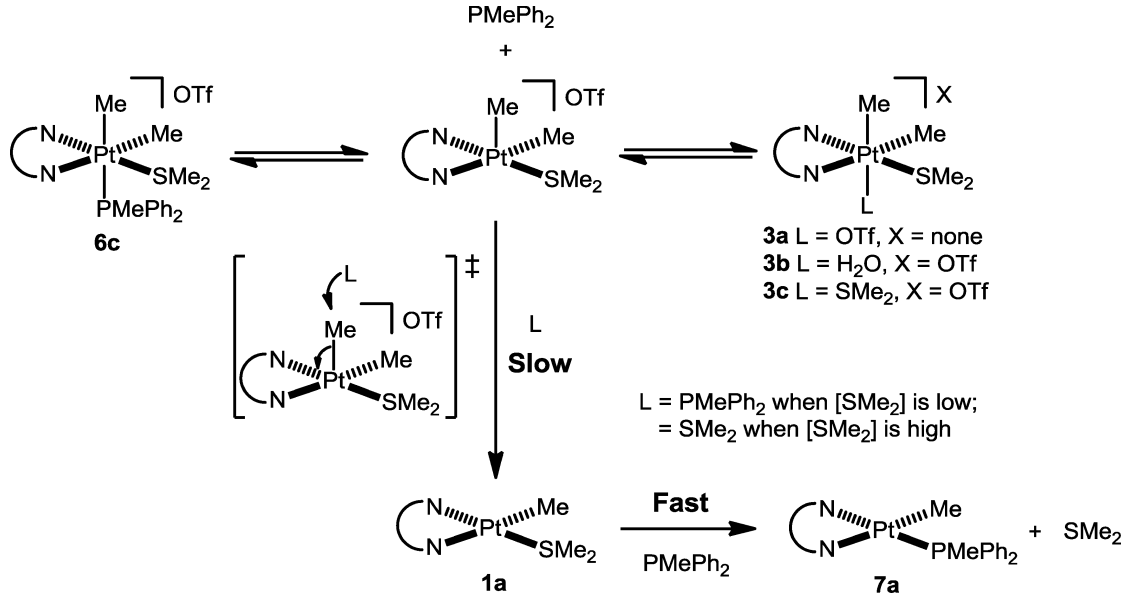

dx.doi.org/10.1021/om400034y | *Organometallics* 2013, 32, 1938−1950

Scheme 3. Proposed Mechanism for the Conversion of 3 to 7b

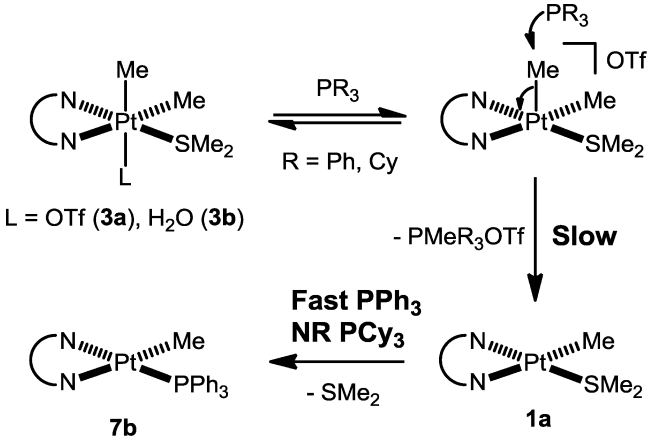

used. The reductive elimination appears to proceed through an S_N2 type two-step process rather than a concerted reductive elimination; because of this, we would expect to see a dependence on the nucleophilicity of phosphine, but this seems to make little difference. The most electrophilic site on the Pt(IV) complex **3** is the Pt itself, so that phosphines preferentially bind to the metal, but this interaction is sterically inhibited when large phosphines are used, allowing them to attack the less electrophilic but more exposed axial methyl group.

Reductive elimination from Pd(IV) and Pt(IV) has been shown to be a versatile method of forming new C−X bonds, but these reactions typically require high temperatures to occur. In this case we are able to form new P−C bonds at room temperature via reductive elimination from Pt(IV). The bond-forming step favors sterically encumbered nucleophiles, which could be a useful method for selective reactions with what would generally be inferior nucleophiles.

EXPERIMENTAL SECTION

General Procedures. Reactions were performed under an atmosphere of dry nitrogen or argon using standard drybox and Schlenk techniques. Argon and nitrogen were purified by passage through columns of BASF R3-11 catalyst and 4 Å molecular sieves. All glassware was oven-dried or flame-dried under vacuum and cooled under a nitrogen atmosphere before use. Methylene chloride, pentane, and diethyl ether were purified under an argon atmosphere by passage through a column of activated alumina.[52] Tetrahydrofuran was freshly distilled from sodium/benzophenone ketyl prior to use. Methylene chloride-d_2 was vacuum-transferred from CaH_2 and degassed by several freeze−pump−thaw cycles. The complexes $Pt_2Me_4(\mu\text{-}SMe_2)_2$[53] and $Pt(SMe)_2MeCl$[53] and the ligand *N*-tolyl-ATI (*N*-tolyl(2-tolylamino)troponimine)[54,55] were synthesized according to published procedures. All other reagents were used as received.

For simplicity, the NMR data for the *N*-tolyl-ATI ligand for all of the complexes have been compiled in Table 3. Crystal data and data collection parameters for **1a**, **3a**, **4a**, **6a**, and **7a** are given in Table 4.

(*N*-tolyl-ATI)Pt(CH$_3$)(SMe$_2$) (1a). A Schlenk flask containing 211.5 mg (0.71 mmol) of *N*-tolyl-ATI in THF was cooled to −78 °C, and 0.31 mL (0.78 mmol, 1.1 equiv) of 2.5 M nBuLi was added slowly. The solution was warmed to room temperature. A solution of 250 mg (0.68 mmol, 0.95 equiv) of $PtMe(SMe_2)_2Cl$ in THF was cannula-transferred to the Schlenk flask containing $[Li]^+[N\text{-tolyl-ATI}]^-$. After 2 h the solvent was removed under vacuum. The resulting product was purified via column chromatography using a silica gel column treated with a 97/3 CH_2Cl_2/NEt_3 solution and a mobile phase of 9/1 hexanes/ethyl acetate to yield 193 mg (0.34 mmol, 48%) of pure **1a**. X-ray-quality crystals were formed by recrystallization from layered pentane on top of a diethyl ether solution of **1a** at −35 °C. ^{1}H NMR (δ, CD_2Cl_2, 400 MHz, 298 K): 2.09 (6H, s, $S(CH_3)_2$, $^3J_{Pt-H}$ = 48 Hz), 0.05 (3H, s, $PtCH_3$, $^2J_{Pt-H}$ = 76 Hz). ^{13}C NMR (δ, CD_2Cl_2, 100 MHz, 298 K): 22.3 ($S(CH_3)_2$), −12.2 ($PtCH_3$, $^1J_{Pt-C}$ = 729 Hz). Anal. Calcd for $C_{24}H_{28}N_2PtS$: C, 50.43; H, 4.94; N, 4.90. Found: C, 50.70; H, 4.89; N, 4.66.

Scheme 4. Divergent Reaction Pathways Based on Phosphine Cone Angle

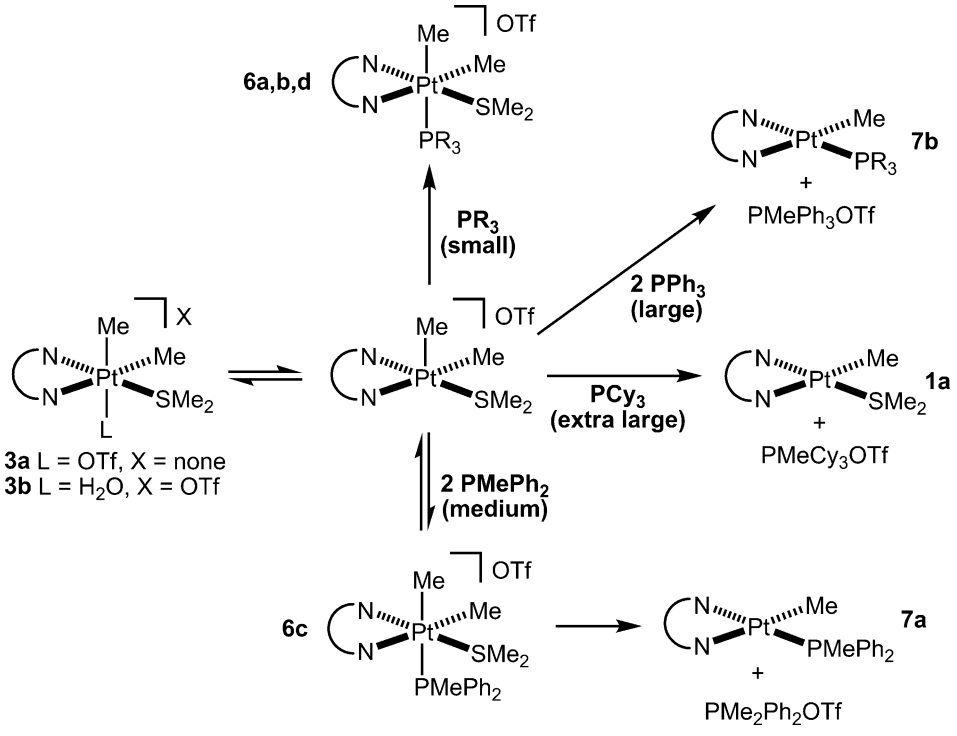

dx.doi.org/10.1021/om400034y | *Organometallics* 2013, 32, 1938−1950

Table 3. ^{1}H and ^{13}C NMR Data for the *N*-tolyl-ATI Ligand of Complexes 1−7

complex	*N*-tolyl-ATI aromatic (δ, ppm)	tolyl methyl (δ, ppm)
1a	^{1}H: 7.29 d, 4H, J_{H-H} = 9 Hz; 6.923 d, 2H, J_{H-H} = 7 Hz; 6.87 d, 2H, J_{H-H} = 6 Hz; 6.805 t, 1H; 6.780 t, 1H; 6.324 d, 1H, J_{H-H} = 11 Hz; 6.219 d, 1H, J_{H-H} = 11 Hz; 6.151 t, 1H	^{1}H: 2.43
	^{13}C: 166.75; 163.93, J_{Pt-C} = 44 Hz; 148.00; 146.97, J_{Pt-C} = 49 Hz; 134.72; 134.57; 131.78; 131.51; 130.41; 130.32; 126.99; 125.50; 119.49; 118.74; 117.69, J_{Pt-C} = 36 Hz	^{13}C: 21.2
1b	^{1}H: 7.30 m, 4H; 6.94 m, 2H; 6.87 d, 2H, J_{H-H} = 8 Hz; 6.787 d, 2H, J_{H-H} = 8 Hz; 6.565 t, 2H; 6.446 t, 1H	^{1}H: 2.42
	^{13}C: 168.4; 165.2; 147.0; 144.2; 135.3; 135.1; 133.5; 133.0; 130.7; 130.4; 126.7; 124.9; 121.5; 119.5; 116.8	^{13}C: 21.1
1c	^{1}H: 7.30 t, 4H; 7.10 d, 2H, J_{H-H} = 8 Hz; 6.99 m, 2H; 6.83 d, 2H, J_{H-H} = 8 Hz; 6.75 d, 1H, J_{H-H} = 12 Hz; 6.48 t, 1H; 6.48 d, 1H, J_{H-H} = 11	^{1}H: 2.42
	^{13}C: 169.0; 164.0; 150.4; 144.8; 135.6; 135.5; 133.3; 133.1; 130.5; 130.4; 127.1; 124.4; 122.3; 119.1; 118.8	^{13}C: 21.0
2	^{1}H: 7.72 d, 1H, J_{H-H} = 7 Hz; 7.50 d, 1H, J_{H-H} = 7 Hz; 7.34 d, 2H, J_{H-H} = 8 Hz; 7.25 d, 2H, J_{H-H} = 7 Hz; 6.87 d, 1H, J_{H-H} = 8 Hz; 6.83 d, 1H, J_{H-H} = 7 Hz; 6.71 t, 1H; 6.66 t, 1H; 6.18 d, 1H, J_{H-H} = 12; 6.01 t; 1H; 5.99 d, 1H, J_{H-H} = 12	^{1}H: 2.41; 2.40
	^{13}C: 165.7, J_{Pt-C} = 14 Hz; 164.7, J_{Pt-C} = 26 Hz; 146.3, J_{Pt-C} = 11 Hz; 144.6; 136.4; 135.7; 133.8; 133.8; 130.8; 130.4; 128.5; 126.9; 120.1, J_{Pt-C} = 10 Hz; 119.9; 118.5; J_{Pt-C} = 22 Hz	^{13}C: 21.2; 21.1
3	^{1}H (RT): 7.33 t, 4H; 7.13 m, 2H; 7.08 m, 2H; 6.91 t, 1H; 6.85 t, 1H; 6.49 d, 1H, J_{H-H} = 11.2 Hz; 6.29 t, 2H	^{1}H: 2.44; 2.41
	^{13}C (RT): 165.9, J_{Pt-C} = 23 Hz; 164.8, J_{Pt-C} = 32 Hz; 146.1; 144.2, J_{Pt-C} = 31 Hz; 136.8; 136.3; 134.23; 134.15; 131.1; 131.0; 127.7; 125.3; 122.0; 120.8; 119.5, J_{Pt-C} = 30 Hz	^{13}C: 21.2
4a	^{1}H: 7.38 m, 4H; 6.93 s-broad, 1H; 6.85 m, 4H; 6.78 t, 1H; 6.36 d, 1H, J_{H-H} = 12 Hz; 6.20 t, 1H; 6.12 d, 1H, J_{H-H} = 11 Hz	^{1}H: 2.45; 2.42.
	^{13}C: 165.9, J_{Pt-C} = 21 Hz; 165.16, J_{Pt-C} = 34 Hz; 145.3; 143.9, J_{Pt-C} = 28 Hz; 135.2; 135.0; 131.7; 131.6; 123.1; 122.1; 121.1; 119.9; 119.6, J_{Pt-C} = 25 Hz	^{13}C: 21.2; 21.1.
4b	^{1}H: 7.42−6.8,16H, $(CH_3)_2C_6H_3NC$ and *N*-tolyl-ATI arom	^{1}H: 2.40 s, 9H, $(CH_3)_2C_6H_3NC$ and ATI tolyl methyl
	^{13}C: 165.7−119.7, $(CH_3)_2C_6H_3NC$ and *N*-tolyl-ATI arom	^{13}C: 21.2; 21.1
5a	^{1}H: 7.33−5.95	^{1}H: 2.42; 2.41
	^{13}C: 165.2; 164.0; 146.1; 144.2; 136.0; 135.3; 133.7; 133.6; 130.3; 128.1; 126.3; 125.0; 119.8; 119.4; 118.0	^{13}C: 20.8, 20.7
5b	^{1}H: 7.29 m, 6H; 6.89 m, 2H; 6.67 t, 1H; 6.61 t, 1H; 6.13 d, 1H, J_{H-H} = 12 Hz; 5.95 t, 1H; 5.92 d, 1H, J_{H-H} = 12 Hz	^{1}H: 2.41; 2.40
	^{13}C: 165.7, J_{Pt-C} = 15 Hz; 164.6; 146.2; 144.6, J_{Pt-C} = 21 Hz; 136.3; 135.6; 134.2; 134.1; 131.1; 127.6; 127.0; 125.1; 119.3 J_{Pt-C} = 8 Hz; 117.6 J_{Pt-C} = 20 Hz	^{13}C: 21.2, 21.1
6a	^{1}H: 7.38 m, 4H; 7.40 d, 1H, J_{H-H} = 8 Hz; 7.00 d, 1H, J_{H-H} = 8 Hz; 6.81 m, 4H; 6.31 d, 1H, J_{H-H} = 12 Hz; 6.20 t, 1H; 6.10 d, 1H, J_{H-H} = 12 Hz	^{1}H: 2.47; 2.45
	^{13}C: 165.9, J_{Pt-C} = 15 Hz; 165.4, J_{Pt-C} = 24 Hz; 146.0, J_{Pt-C} = 8 Hz; 143.4, J_{Pt-C} = 26 Hz; 137.8; 137.4; 135.2; 134.9; 131.9, J_{P-C} = 51 Hz; 131.5, J_{Pt-C} = 86 Hz; 127.6; 126.4; 122.4, J_{P-C} = 3 Hz; 122.0, J_{P-C} = 3 Hz; 120.8, J_{P-C} = 3 Hz.	^{13}C: 21.2, 21.1
6b	^{1}H: 7.50 −6.04, 18H, PtPPh and *N*-tolyl-ATI arom	^{1}H: 2.39
	^{13}C: 166.3−121.2, PtPPh and *N*-tolyl-ATI arom	^{13}C: 21.2, 21.0
6c	^{1}H: 7.76−5.93, 23H, $PtPPh_2$ and *N*-tolyl-ATI arom	^{1}H: 2.38; 2.35
	^{13}C: 164.7−118.6, $PtPPh_2$ and *N*-tolyl-ATI arom	^{13}C: 20.5, 20.4
6d	^{1}H: 7.32 m, 6H; 6.96 m, 7H; 6.8 dd, 1H, J_{H-H} = 12, 2 Hz; 6.74 dd, 1H, J_{H-H} = 12, 2 Hz; 6.34 dd, 1H, J_{H-H} = 12, 2 Hz; 6.10 dd, 1H, J_{H-H} = 12, 2 Hz	^{1}H: 2.42; 2.40
	^{13}C: 165.9, J_{Pt-C} = 18 Hz; 165.3, J_{Pt-C} = 32 Hz; 144.7; 143.3, J_{Pt-C} = 30 Hz; 137.1; 136.4; 134.8; 134.5; 131.1; 130.8; 127.2; 126.4; 125.0; 124.8; 122.6; 121.8; 121.3; 119.4; 119.4	^{13}C: 20.7; 20.6
7a	^{1}H: 7.41−6.13, 23H, $PtPPh_2$ and *N*-tolyl-ATI arom	^{1}H: 2.37; 2.31
	^{13}C: 166.8−114.7, $PtPPh_2$ and *N*-tolyl-ATI arom	^{13}C: 21.0, 20.9
7b	^{1}H: 7.49−5.98, 28H, PPh_3 and *N*-tolyl-ATI arom	^{1}H: 2.38; 2.31
	^{13}C: 167.0−117.1, PPh_3 and *N*-tolyl-ATI arom	^{13}C: 21.0, 20.8

(*N*-tolyl-ATI)Pt(CH_3)(η^2-C_2H_4) (1b). A Schlenk flask containing 162 mg (0.54 mmol) of *N*-tolyl-ATI in THF was cooled to −78 °C, and 0.24 mL (0.59 mmol, 1.1 equiv) of nBuLi was added slowly. The solution was warmed to room temperature. A solution of 200 mg (0.54 mmol, 1.0 equiv) of $PtMe(SMe_2)_2Cl$ in THF was cannula-transferred to the Schlenk flask containing $[Li]^+[N\text{-tolyl-ATI}]^-$. The solution was stirred for 30 min before ethylene gas was bubbled into the solution. After 30 min of bubbling, the solvent was removed under vacuum, and the resulting product was purified via column chromatography using a silica gel column treated with a 97/3 CH_2Cl_2/NEt_3 solution and a mobile phase of 8/2 hexanes/CH_2Cl_2. The first band contained the product **1b**, along with free ligand. This product was collected and reduced to dryness before being chromatographed again using a silica gel column with a mobile phase of 100% CH_2Cl_2 to yield 72 mg (0.13 mmol, 24%) of pure **1b**. ^{1}H NMR (δ, CD_2Cl_2, 400 MHz, 298 K): 2.89 (4H, s, Pt(η^2-CH_2═CH_2), $^2J_{Pt-H}$ = 58 Hz), −0.27 (3H, s, PtCH_3, $^2J_{Pt-H}$ = 71 Hz). ^{13}C NMR (δ, CD_2Cl_2, 100 MHz, 298 K): 59.5 (Pt(η^2-CH_2═CH_2), $^1J_{Pt-C}$ = 204 Hz), −7.2 ($PtCH_3$, $^1J_{Pt-C}$ = 689 Hz). Anal. Calcd for $C_{25}H_{29}N_2Pt$: C, 53.90; H, 4.65; N, 4.98. Found: C, 53.62; H, 4.88; N, 5.21.

(*N*-tolyl-ATI)Pt(CH_3)(CO) (1c). The same procedure as for **1b** was used to prepare **1c**, but CO was bubbled through the solution rather than ethylene to yield 76 mg of **1c** (0.14 mmol, 26%). IR (hexanes): ν_{CO} 2062 cm^{-1}. ^{1}H NMR (δ, CD_2Cl_2, 400 MHz, 298 K): 0.25 (3H, s, PtCH_3, $^2J_{Pt-H}$ = 70 Hz). ^{13}C NMR (δ, CD_2Cl_2, 100 MHz, 298 K): 169.9(Pt-CO); −15.3 ($PtCH_3$). Anal. Calcd for $C_{23}H_{22}N_2OPt\cdot{}^1/_2C_6H_{14}\cdot{}^1/_2CH_2Cl_2$: C, 51.04; H, 4.93; N, 4.49. Found: C, 51.25; H, 4.53; N, 4.27.

(*N*-tolyl-ATI)Pt(CH_3)$_2$(I)(SMe_2) (2). A Schlenk flask containing 30 mg (0.052 mmol) of **1a** in CH_2Cl_2 was cooled to −78 °C, and 4 μL of MeI (0.063 mmol, 1.2 equiv) was syringed into the flask. The solution was stirred for 5 min before the flask was warmed to room temperature, and then it was stirred for an additional 15 min. The solvent was removed in vacuo, and the resulting product was purified via flash column chromatography using an alumina column with a mobile phase of 100% CH_2Cl_2 to yield 16 mg (0.022 mmol, 42%) of pure **2**. ^{1}H NMR (δ, CD_2Cl_2, 500 MHz, 298 K): 2.34 (3H, s, S(CH_3)$_2$,

dx.doi.org/10.1021/om400034y | *Organometallics* 2013, 32, 1938−1950

Table 4. Crystal Data and Data Collection Parameters for (*N*-tolyl-ATI)Pt(CH_3)(SMe_2) (1a), (*N*-tolyl-ATI)Pt(CH_3)$_2$(OH_2)(SMe_2)[OTf] (3a), (*N*-tolyl-ATI)Pt(CH_3)$_2$(*t*BuNC)(SMe_2)[OTf] (4a), and (*N*-tolyl-ATI)Pt(CH_3)$_2$(PMe_3)(SMe_2)[OTf] (6a)

	1a	3a	4a	6a	7a
empirical formula	$C_{24}H_{28}N_2PtS$	$C_{26}H_{33}F_3N_2O_4PtS_2$	$C_{31}H_{40}F_3N_3O_3PtS_2$	$C_{29}H_{42}F_3N_2O_4PPtS_2$	$C_{35}H_{35}N_2PPt$
fw	571.63	753.75	818.87	829.83	709.71
temp, K	100(2)	100(2)	100(2)	100(2)	100(2)
wavelength, Å	1.54178	1.54178	0.71073	1.54178	1.54178
cryst syst	monoclinic	monoclinic	triclinic	monoclinic	triclinic
space group	$P2_1/n$	$P2_1/c$	$P\bar{1}$	$P2_1/c$	$P\bar{1}$
a, Å	12.6651(8)	11.6760(5)	9.3286(2)	13.5687(7)	10.2555(8)
b, Å	9.9737(6)	19.1569(8)	12.9106(2)	19.0331(12)	12.2417(9)
c, Å	18.3405(10)	12.6460(5)	14.9100(3)	13.5212(7)	12.6678(10)
α, deg	90	90	83.989(1)	90	95.950(4)
β, deg	106.824(4)	94.933(3)	73.274(1)	110.214(2)	100.623(5)
γ, deg	90	90	83.268(1)	90	110.784(4)
V, Å^3	2217.6(2)	2818.1(2)	1703.13(6)	3276.8(3)	1436.4(2)
Z	4	4	2	4	2
ρ_{calcd}, Mg/m^3	1.712	1.777	1.597	1.682	1.641
μ, mm^{-1}	12.787	11.178	4.293	10.121	9.857
F(000)	1120	1488	816	1656	704
cryst size, mm^3	0.15 × 0.15 × 0.05	0.10 × 0.10 × 0.10	0.20 × 0.15 × 0.05	0.08 × 0.08 × 0.40	0.05 × 0.10 × 0.23
2θ range, deg	3.78−65.53	3.80−70.13	2.06−30.59	3.47−66.24	3.61−66.58
index ranges	$-14 \le h \le 14$	$-13 \le h \le 13$	$-13 \le h \le 13$	$-16 \le h \le 16$	$-9 \le h \le 11$
	$0 \le k \le 11$	$0 \le k \le 23$	$-17 \le k \le 18$	$-22 \le k \le 17$	$-14 \le k \le 14$
	$0 \le l \le 21$	$0 \le l \le 15$	$-21 \le l \le 21$	$-16 \le l \le 15$	$-14 \le l \le 15$
no. of rflns collected	88713	5178	45821	25356	11579
no. of indep rflns	3815 (*R*(int) = 0.0493)	5178 (*R*(int) = 0.0000)	10430 (*R*(int) = 0.0554)	5742 (*R*(int) = 0.0340)	4799 (*R*(int) = 0.0767)
no. of data/restraints/params	3815/0/261	5178/0/360	10430/0/398	5742/3/402	4799/0/356
goodness of fit on F^2	1.094	1.132	1.035	1.160	1.007
final *R* indices ($I > 2\sigma(I)$)	R1 = 0.0507, wR2 = 0.1113	R1 = 0.0475, wR2 = 0.1000	R1 = 0.0346, wR2 = 0.0614	R1 = 0.0586, wR2 = 0.1444	R1 = 0.0499, wR2 = 0.1207
R indices (all data)	R1 = 0.0584, wR2 = 0.1145	R1 = 0.0568, wR2 = 0.1036	R1 = 0.0479, wR2 = 0.0654	R1 = 0.0618, wR2 = 0.1467	R1 = 0.0641, wR2 = 0.1280

$^3J_{Pt-H}$ = 32 Hz), 1.79 (3H, s, S(CH_3)$_2$, $^3J_{Pt-H}$ = 35 Hz), 1.51 (3H, s, PtCH_3, $^2J_{Pt-H}$ = 71 Hz), 0.71 (3H, s, PtCH_3, $^2J_{Pt-H}$ = 64 Hz). ^{13}C NMR (δ, CD_2Cl_2, 125 MHz, 298 K): 24.7 (S(CH_3)$_2$), 19.0 (S(CH_3)$_2$), 13.8 (PtCH_3, $^1J_{Pt-C}$ = 474 Hz), 1.7 (PtCH_3, $^1J_{Pt-C}$ = 449 Hz). Anal. Calcd for $C_{25}H_{31}IN_2PtS$: C, 42.43; H, 4.35; N, 4.28. Found: C, 42.08; H, 4.38; N, 3.93.

Preparation of Mixtures of [(*N*-tolyl-ATI)Pt(CH_3)$_2$(OH_2)(SMe_2)][OTf] (3a) and (*N*-tolyl-ATI)Pt(CH_3)$_2$(O_3SCF_3)(SMe_2) (3b). A Schlenk flask containing 145 mg (0.25 mmol) of **1a** was cooled to −78 °C, and 34 μL of MeOTf (0.30 mmol, 1.2 equiv) was syringed in. The solution was allowed to stirred for 5 min before the flask was warmed to room temperature and stirred for 15 min more. The solvent was removed under vacuum. The resulting product was purified via flash column chromatography using an alumina column with a mobile phase of 100% CH_3CN. The solid was washed with pentanes and dried to yield 148 mg of **3a**,**b**. X-ray-quality crystals of **3a** were formed by slow evaporation of a solution of **3a** in methylene chloride at room temperature. ^{1}H NMR (δ, CD_2Cl_2, 400 MHz, 298 K): 1.98 (6H, br s, S(CH_3)$_2$, $^3J_{Pt-H}$ = 32 Hz), 1.05 (6H, br s, PtCH_3, $^2J_{Pt-H}$ = 71 Hz). ^{13}C NMR (δ, CD_2Cl_2, 100 MHz, 298 K): 19.9 (br, S(CH_3)$_2$); 3.1 (br, PtCH_3, $^1J_{Pt-C}$ = 619 Hz). Elemental analysis could not be performed on these compounds, as they are produced as an equilibrium mixture.

[(*N*-tolyl-ATI)Pt(CH_3)$_2$(CNBu^t)(SMe_2)][OTf] (4a). A Schlenk flask containing 40 mg (0.070 mmol) of **1a** was purged with nitrogen, and dry CH_2Cl_2 was syringed into the flask. The solution was cooled to −78 °C, and 15.8 μL (0.144 mmol, 2 equiv) of MeOTf was syringed in to synthesize **3** in situ. The reaction mixture was warmed to room temperature, and the solvent was removed under vacuum. Dry CH_2Cl_2 was syringed into the flask followed by 11.9 μL (0.105 mmol, 1.5 equiv) of *tert*-butyl isocyanide. The solution was stirred for 2 h before the solvent was removed under vacuum. The resulting product was purified via flash column chromatography using an alumina column with a mobile phase of 100% CH_2Cl_2 to wash off organic byproducts followed by 100% CH_3CN. The CH_3CN fraction was collected and reduced to dryness and the residue triturated with pentanes to yield 35 mg (0.043 mmol, 67%) of pure **4a**. X-ray-quality crystals were formed by slow evaporation of a solution of **4a** in methylene chloride at room temperature. IR (CH_2Cl_2): $\nu_{C\equiv N}$ 2217 cm^{-1}. ^{1}H NMR (δ, CD_2Cl_2, 400 MHz, 298 K): 2.22 (3H, s, S(CH_3)$_2$, $^3J_{Pt-H}$ = 34 Hz), 2.09 (3H, s, S(CH_3)$_2$, $^3J_{Pt-H}$ = 37 Hz), 1.64 (9H, s, CN-*Bu*^{t}), 1.18 (3H, s, PtCH_3, $^2J_{Pt-H}$ = 62 Hz), 0.46 (3H, s, PtCH_3, $^2J_{Pt-H}$ = 62 Hz). ^{13}C NMR (δ, CD_2Cl_2, 100 MHz, 298 K): 30.2 (CN-*Bu*^{t}), 24.8 (S(CH_3)$_2$), 19.6 (S(CH_3)$_2$), 8.4 (PtCH_3, $^1J_{Pt-C}$ =500 Hz), 2.1 (PtCH_3, $^1J_{Pt-C}$ = 536 Hz). Anal. Calcd for $C_{31}H_{40}F_3N_3O_3PtS_2$: C, 45.47; H, 4.92; N, 5.13. Found: C, 45.71; H, 4.83; N, 5.23.

[(*N*-tolyl-ATI)Pt(CH_3)$_2$($CNC_6H_3Me_2$)(SMe_2)][OTf] (4b). The same procedure as for **4a** was used to prepare **4b**, but 2,6-dimethylphenyl isocyanide was used instead of *tert*-butyl isocyanide. The yield of **4b** was 57 mg (0.066 mmol, 94%). IR (CH_2Cl_2): $\nu_{C\equiv N}$ 2196 cm^{-1}. ^{1}H NMR (δ, CD_2Cl_2, 500 MHz, 298 K): 7.42−6.8 (16H, m, (CH_3)$_2C_6H_3NC$ and *N-tolyl-ATI arom*), 2.45 (3H, s, (CH_3)$_2C_6H_3NC$), 2.40 (9H, s, (CH_3)$_2C_6H_3NC$ and tolyl methyls), 2.34 (3H, s, S(CH_3)$_2$, $^3J_{Pt-H}$ = 34 Hz), 2.14 (3H, s, S(CH_3)$_2$, $^3J_{Pt-H}$ = 37 Hz), 1.31 (3H, s, PtCH_3, $^2J_{Pt-H}$ = 63 Hz), 0.61 (3H, s, PtCH_3, $^2J_{Pt-H}$ = 62 Hz). ^{13}C NMR (δ, CD_2Cl_2, 125 MHz, 298 K): 165.7−119.7 ((CH_3)$_2C_6H_3NC$ and *N-tolyl-ATI arom*), 131.7 (br, C≡N), 25.3 (S(CH_3)$_2$), 19.5 (S(CH_3)$_2$), 19.0 ((CH_3)$_2C_6H_3NC$)), 8.5 (PtCH_3, $^1J_{Pt-C}$ = 400 Hz), 1.9 (PtCH_3, $^1J_{Pt-C}$ = 430 Hz). Anal.

dx.doi.org/10.1021/om400034y | *Organometallics* 2013, 32, 1938−1950

Calcd for $C_{35}H_{40}F_3N_3O_3PtS_2$: C, 48.49; H, 4.65; N, 4.85. Found: C, 48.47; H, 4.46; N, 4.77.

(*N*-tolyl-ATI)Pt(CH_3)$_2$(N_3)(SMe_2) (5a). A Schlenk flask containing 20 mg (0.035 mmol) of **1a** was purged with nitrogen, and dry CH_2Cl_2 was added to the flask. The solution was cooled to −78 °C, and 7.9 μL (0.07 mmol, 2 equiv) of MeOTf was syringed in to synthesize **3** in situ. The flask was warmed to room temperature, and the solvent was removed under vacuum. A large excess of NaN_3 was added to the Schlenk flask. Dry CH_2Cl_2 was syringed into the flask and the solution stirred for 18 h. The solvent was removed under vacuum. The resulting product was purified via flash column chromatography using an alumina column with a mobile phase of 100% CH_2Cl_2 to remove excess NaN_3 and organic byproducts followed by 100% CH_3CN. The CH_3CN fraction was collected and reduced to dryness and the residue triturated with pentanes to yield 12 mg (0.019 mmol, 54%) of pure **5a**. IR (CH_2Cl_2): ν_{N_3} 2038 cm^{-1}. ^{1}H NMR (δ, CD_2Cl_2, 400 MHz, 298 K): 1.97 (3H, s, S(CH_3)$_2$, $^3J_{Pt-H}$ = 31 Hz), 1.88 (3H, s, S(CH_3)$_2$, $^3J_{Pt-H}$ = 36 Hz), 1.07 (3H, s, PtCH_3, $^2J_{Pt-H}$ = 70 Hz), 0.38 (3H, s, PtCH_3, $^2J_{Pt-H}$ = 62 Hz). ^{13}C NMR (δ, CD_2Cl_2, 100 MHz, 298 K): 19.8 (S(CH_3)$_2$), 18.0 (S(CH_3)$_2$), 3.4 (PtCH$_3$), −4.33 (PtCH$_3$). A satisfactory elemental analysis was not obtained; therefore, the purity was determined by ^{1}H NMR.

(*N*-tolyl-ATI)Pt(CH_3)$_2$(CN)(SMe_2) (5b). The same procedure as for **5a** was used to prepare **5b**, but NaCN was used instead of NaN_3 to give 5.8 mg of the product (0.096 mmol, 27.3%). IR (CH_2Cl_2): $\nu_{C\equiv N}$ 2301 cm^{-1}. ^{1}H NMR (δ, CD_2Cl_2, 500 MHz, 298 K): 2.23 (3H, s, S(CH_3)$_2$, $^3J_{Pt-H}$ = 35 Hz), 1.97 (3H, s, S(CH_3)$_2$, $^3J_{Pt-H}$ = 35 Hz), 0.69 (3H, s, PtCH_3, $^2J_{Pt-H}$ = 56 Hz), 0.39 (3H, s, PtCH_3, $^2J_{Pt-H}$ = 64 Hz). ^{13}C NMR (δ, CD_2Cl_2, 125 MHz, 298 K): 24.5 (S(CH_3)$_2$), 19.1 (S(CH_3)$_2$), 3.3 (PtCH$_3$, $^1J_{Pt-C}$ = 367 Hz), 0.0 (PtCH$_3$, $^1J_{Pt-C}$ = 442 Hz). Anal. Calcd for $C_{26}H_{31}N_3PtS$: C, 50.97; H, 5.10; N, 6.86. Found: C, 51.19; H, 4.89; N, 6.71.

[(*N*-tolyl-ATI)Pt(CH_3)$_2$(PMe_3)(SMe_2)][OTf] (6a). In the glovebox, in a preweighed vial containing 20 mg (0.035 mmol) of **1a** was added CH_2Cl_2. MeOTf (4.6 μL, 0.042 mmol, 1.2 equiv) was syringed in to synthesize **3** in situ. The mixture was allowed to react for 5 min, the solvent was removed under vacuum, and the residue was triturated with hexanes and dried to remove any excess MeOTf. The residue was dissolved in CH_2Cl_2, and 4.3 μL (0.042 mmol, 1.2 equiv) of PMe_3 was syringed into the vial to form a red solution. The solution was allowed to react for 5 min, and the solvent and excess PMe_3 were removed under vacuum followed by trituration with hexanes to give **6a** in 99% yield (28 mg, 0.035 mmol). X-ray-quality crystals were formed by recrystallization from layering hexanes on top of a solution of **6a** in methylene chloride at −35 °C. ^{1}H NMR (δ, CD_2Cl_2, 500 MHz, 298 K): 2.23 (3H, br s, S(CH_3)$_2$, $^3J_{Pt-H}$ = 35 Hz), 1.58 (9H, d, P(CH_3)$_3$, 3H, S(CH_3)$_2$), 1.36 (3H, d, PtCH_3, $^2J_{Pt-H}$ = 57 Hz, $^3J_{P-H}$ = 9 Hz), 0.45 (3H, d, PtCH_3, $^2J_{Pt-H}$ = 62 Hz, $^3J_{P-H}$ = 8 Hz). ^{13}C NMR (δ, CD_2Cl_2, 125 MHz, 298 K): 21.6 (S(CH_3)$_2$), 18.4 (S(CH_3)$_2$), 12.5 (PtCH$_3$, $^1J_{Pt-C}$ = 370 Hz, $^2J_{P-C}$ = 103 Hz), 11.2 (P(CH_3)$_3$, $^1J_{P-C}$ = 20 Hz), 3.08 (PtCH$_3$, $^1J_{Pt-C}$ = 440 Hz). ^{31}P NMR (δ, CD_2Cl_2, 162 MHz, 298 K): −30.0 (*P*Me$_3$, $^1J_{Pt-P}$ = 1101 Hz). Anal. Calcd for $C_{29}H_{40}F_3N_2O_3PPtS_2$: C, 42.91; H, 4.97; N, 3.45. Found: C, 42.88; H, 4.73; N, 3.42.

[(*N*-tolyl-ATI)Pt(CH_3)$_2$($PPhMe_2$)(SMe_2)][OTf] (6b). The same procedure as for **6a** was used to prepare **6b**, but $PPhMe_2$ was used instead of PMe_3; **6b** was obtained in 97% yield (30 mg, 0.034 mmol). ^{1}H NMR (δ, CD_2Cl_2, 500 MHz, 298 K): 7.50−6.04 (18H, Ar, P*Ph*Me$_2$ and *N-tolyl-ATI arom*), 1.99 (3H, br s, S(CH_3)$_2$), 1.90 (3H, d, PtP(CH_3)$_2$), 1.77 (3H, d, P(CH_3)$_2$), 1.36 (3H, d, PtCH_3, $^2J_{Pt-H}$ = 59 Hz, $^3J_{P-H}$ = 8 Hz), 1.08 (3H, br s, S(CH_3)$_2$), 0.46 (3H, d, PtCH_3 Eq, $^2J_{Pt-H}$ = 62 Hz, $^3J_{P-H}$ = 8 Hz). ^{13}C NMR (δ, CD_2Cl_2, 125 MHz, 298 K): 166.3−121.2 (P*Ph*Me$_2$ and *N-tolyl-ATI arom*), 13.5 (PtCH$_3$, $^2J_{P-C}$ = 100 Hz), 10.4 (S(CH_3)$_2$), 10.2 (PPh(CH_3)$_2$, $^1J_{P-C}$ = 4 Hz), 10.1 (S(CH_3)$_2$), 3.7 (PtCH$_3$). ^{31}P NMR (δ, CD_2Cl_2, 162 MHz, 298 K): −24.1 (*P*PhMe$_2$, $^1J_{Pt-P}$ = 1004 Hz). Anal. Calcd for $C_{34}H_{42}F_3N_2O_3PPtS_2$: C, 46.73; H, 4.84; N, 3.21. Found: C, 46.41; H, 4.75; N, 3.10.

[(*N*-tolyl-ATI)Pt(CH_3)$_2$(PPh_2Me)(SMe_2)][OTf] (6c). The same procedure as for **6a** was used to prepare **6c**, but PPh_2Me was used instead of PMe_3, and the reaction mixture was kept at 0 °C at all times. **6c** was not isolated, as it begins to form **7a** after being synthesized. ^{1}H NMR (δ, CD_2Cl_2, 400 MHz, 298 K): 1.98 (3H, d, P(CH_3)), 1.91 (3H, br s, S(CH_3)$_2$), 1.54 (3H, d, Pt(CH_3), $^2J_{Pt-H}$ = 61 Hz, $^3J_{P-H}$ = 8 Hz), 1.23 (3H, br s, S(CH_3)$_2$), 0.50 (3H, d, Pt(CH_3), $^2J_{Pt-H}$ = 62 Hz, $^3J_{P-H}$ = 8 Hz). ^{13}C NMR (δ, CD_2Cl_2, 125 MHz, 193 K): 164.7−118.6 (P*Ph*$_2$Me and *N-tolyl-ATI arom*), 18.8 (S(CH_3)$_2$), 16.5 (S(CH_3)$_2$), 13.8 (PtCH$_3$, $^2J_{P-C}$ = 97 Hz), 7.4 (PPh$_2$(CH_3), $^1J_{P-C}$ = 20 Hz), 4.4 (PtCH$_3$). ^{31}P NMR (δ, CD_2Cl_2, 162 MHz, 298 K): −23.8 (*P*Ph$_2$Me, $^1J_{Pt-P}$ = 877 Hz).

[(*N*-tolyl-ATI)Pt(CH_3)$_2$($P(OMe)_3$)(SMe_2)][OTf] (6d). The same procedure as for **6a** was used to prepare **6d**, but P(OMe)$_3$ was used instead of PMe_3; **6d** was obtained in 96% yield (29 mg, 0.034 mmol). ^{1}H NMR (δ, CD_2Cl_2, 400 MHz, 298 K): 3.88 (9H, d, P(OCH_3)$_3$, $^3J_{P-H}$ = 10 Hz), 2.18 (3H, br s, S(CH_3)$_2$, $^3J_{Pt-H}$ = 32 Hz), 1.82 (3H, S(CH_3)$_2$, $^3J_{Pt-H}$ = 36 Hz), 1.17 (3H, d, PtCH_3, $^2J_{Pt-H}$ = 57 Hz, $^3J_{P-H}$ = 12 Hz), 0.45 (3H, d, PtCH_3, $^2J_{Pt-H}$ = 63 Hz, $^3J_{P-H}$ = 9 Hz). ^{13}C NMR (δ, CD_2Cl_2, 100 MHz, 298 K): 54.7 (P(OCH_3)$_3$, $^1J_{P-C}$ = 12 Hz), 22.5 (S(CH_3)$_2$), 18.9 (S(CH_3)$_2$), 13.6 (PtCH$_3$, $^2J_{P-C}$ = 189 Hz), 2.2 (PtCH$_3$, $^1J_{Pt-C}$ = 536 Hz). ^{31}P NMR (δ, CD_2Cl_2, 162 MHz, 298 K): 83.2 (*P*(OMe)$_3$, $^1J_{Pt-P}$ = 1963 Hz).

(*N*-tolyl-ATI)Pt(CH_3)(PPh_2Me) (7a). Compound **6c** was formed from 20 mg (0.035 mmol) of **1a** by the procedure detailed above and was stirred at room temperature for 4 days and converted completely to **7a**. The reaction mixture can be heated to increase the rate of conversion, and **6c** will completely convert to **7a** in 2 days if heated to 40 °C in CH_2Cl_2. The resulting product was purified via flash column chromatography using an alumina column with a mobile phase of 100% CH_2Cl_2, which was collected, reduced to dryness, and triturated with pentanes to yield pure **7a** as a yellow powder in 88% yield (22 mg, 0.031 mmol). X-ray-quality crystals were formed by slow evaporation of a solution of **7a** in methylene chloride at room temperature. ^{1}H NMR (δ, CD_2Cl_2, 500 MHz, 298 K): 7.41−6.13 (23H, P*Ph*$_2$CH$_3$ and *N-tolyl-ATI arom*), 1.04 (3H, d, PPh$_2$(CH_3), $^2J_{P-H}$ = 10 Hz), −0.035 (3H, d, PtCH_3, $^2J_{Pt-H}$ = 69 Hz, $^3J_{P-H}$ = 5 Hz). ^{13}C NMR (δ, CD_2Cl_2, 125 MHz, 298 K): 166.8−114.7 (P*Ph*$_2$(CH_3) and *N-tolyl-ATI arom*), 12.1 (PPh$_2$(CH_3), $^1J_{P-C}$ = 39 Hz), −10.1 (PtCH$_3$, $^2J_{P-C}$ = 10). ^{31}P NMR (δ, CD_2Cl_2, 162 MHz, 298 K): 1.6 (*P*Ph$_2$(CH_3), $^1J_{Pt-P}$ = 3979 Hz).

(*N*-tolyl-ATI)Pt(CH_3)(PPh_3) (7b). An NMR tube containing 7.6 mg (0.013 mmol) of **1a** was purged with nitrogen, and dry CH_2Cl_2 was syringed into the NMR tube. The solution was cooled to −78 °C, and 3 μL (0.026 mmol, 2 equiv) of MeOTf was syringed into the NMR tube to synthesize **3** in situ. The reaction mixture was warmed to room temperature, and the solvent was removed under vacuum. A large excess of PPh_3 was added to the NMR tube. Dry CD_2Cl_2 was added to form a red solution. The solution was stirred for 2 h. The resulting product was purified via flash column chromatography using an alumina column with a mobile phase of 100% CH_2Cl_2, which was collected, reduced to dryness, and triturated with pentanes to give pure **7b** in 95% yield (9.2 mg, 0.033 mmol) as a yellow powder. ^{1}H NMR (δ, CD_2Cl_2, 500 MHz, 298 K): 7.49−5.98 (28H, P*Ph*$_3$ and *N-tolyl-ATI arom*), −0.33 (3H, d, Pt(CH_3), $^2J_{Pt-H}$ = 69 Hz, $^3J_{P-H}$ = 5 Hz). ^{13}C NMR (δ, CD_2Cl_2, 125 MHz, 298 K): 167.0−117.1 (P*Ph*$_3$ and *N-tolyl-ATI arom*), −7.7 (PtCH$_3$, $^1J_{Pt-P}$ = 9 Hz). ^{31}P NMR (δ, CD_2Cl_2, 162 MHz, 298 K): 18.8 (*P*Ph$_3$, $^1J_{Pt-P}$ = 4134 Hz).

■ ASSOCIATED CONTENT

Ⓢ Supporting Information

CIF files giving crystallographic data for complexes **1a**, **3a**, **4a**, **6a**, and **7a**. This material is available free of charge via the Internet at http://pubs.acs.org.

■ AUTHOR INFORMATION

Corresponding Author

*E-mail: joetemp@unc.edu (J.L.T.); n.west@usciences.edu (N.M.W.).

Notes

The authors declare no competing financial interest.

■ ACKNOWLEDGMENTS

This work was made possible by funding from the NSF (CHE-1058675) and by funding from the University of the Sciences in Philadelphia.

■ REFERENCES

(1) Hartwig, J. F. *Nature* **2008**, *455*, 314.
(2) Stahl, S. S.; Labinger, J. A.; Bercaw, J. E. *Angew. Chem., Int. Ed.* **1998**, *37*, 2181.
(3) Dick, A. R.; Hull, K. L.; Sanford, M. S. *J. Am. Chem. Soc.* **2004**, *126*, 2300.
(4) Dick, A. R.; Sanford, M. S. *Tetrahedron* **2006**, *62*, 2439.
(5) Gol'dshleger, N. F.; Es'kova, V. V.; Shilov, A. E.; Shteinman, A. A. *Russ. J. Phys. Chem.* **1972**, *46*, 785.
(6) Crumpton-Bregel, D. M.; Goldberg, K. I. *J. Am. Chem. Soc.* **2003**, *125*, 9442.
(7) Pawlikowski, A. V.; Getty, A. D.; Goldberg, K. I. *J. Am. Chem. Soc.* **2007**, *129*, 10382.
(8) Dick, A. R.; Kampf, J. W.; Sanford, M. S. *J. Am. Chem. Soc.* **2005**, *127*, 12790.
(9) Racowski, J. M.; Sanford, M. S. *Top. Organomet. Chem.* **2011**, *35*, 61.
(10) Vedernikov, A. N. *Acc. Chem. Res.* **2011**, *45*, 803.
(11) Oloo, W.; Zavalij, P. Y.; Zhang, J.; Khaskin, E.; Vedernikov, A. N. *J. Am. Chem. Soc.* **2010**, *132*, 14400.
(12) Zhao, Y.-L.; Wu, G.-J.; Li, Y.; Gao, L.-X.; Han, F.-S. *Chem. Eur. J.* **2012**, *18*, 9622.
(13) Schwan, A. L. *Chem. Soc. Rev.* **2004**, *33*, 218.
(14) Kondo, T.; Mitsudo, T.-a. *Chem. Rev.* **2000**, *100*, 3205.
(15) Eichman, C. C.; Stambuli, J. P. *Molecules* **2011**, *16*, 590.
(16) Barbaro, P.; Peruzzini, M.; Ramirez, J. A.; Vizza, F. *Organometallics* **1999**, *18*, 4237.
(17) Xu, Y.; Zhang, J. *J. Chem. Soc., Chem. Commun.* **1986**, *0*, 1606.
(18) Font, M.; Parella, T.; Costas, M.; Ribas, X. *Organometallics* **2012**, *31*, 7976.
(19) Fekl, U.; Goldberg, K. I. In *Advances In Inorganic Chemistry: Including Bioinorganic Studies*; Sykes, A. G., Ed.; Academic Press: San Diego, CA, 2003; Vol. *54*, p 259.
(20) Fekl, U.; Kaminsky, W.; Goldberg, K. I. *J. Am. Chem. Soc.* **2003**, *125*, 15286.
(21) West, N. M.; White, P. S.; Templeton, J. L. *J. Am. Chem. Soc.* **2007**, *129*, 12372.
(22) Williams, T. J.; Caffyn, A. J. M.; Hazari, N.; Oblad, P. F.; Labinger, J. A.; Bercaw, J. E. *J. Am. Chem. Soc.* **2008**, *130*, 2418.
(23) Bercaw, J. E.; Hazari, N.; Labinger, J. A.; Oblad, P. E. *Angew. Chem., Int. Ed.* **2008**, *47*, 9941.
(24) Roesky, P. W. *Chem. Soc. Rev.* **2000**, *29*, 335.
(25) Dias, H. V. R.; Wang, Z. Y.; Jin, W. C. *Coord. Chem. Rev.* **1998**, *176*, 67.
(26) Brasen, W. R.; Holmquist, H. E.; Benson, R. E. *J. Am. Chem. Soc.* **1961**, *83*, 3125.
(27) Vedernikov, A. N. *Curr. Org. Chem.* **2007**, *11*, 1401.
(28) Crabtree, R. H. *J. Organomet. Chem.* **2004**, *689*, 4083.
(29) Labinger, J. A.; Bercaw, J. E. *Nature* **2002**, *417*, 507.
(30) Graham, D. C.; Cavell, K. J.; Yates, B. F. *Dalton Trans.* **2005**, 1093.
(31) van Leeuwen, P.; Kamer, P. C. J.; Reek, J. N. H.; Dierkes, P. *Chem. Rev.* **2000**, *100*, 2741.
(32) Freixa, Z.; van Leeuwen, P. *Dalton Trans.* **2003**, 1890.
(33) Zhang, F. B.; Prokopchuk, E. M.; Broczkowski, M. E.; Jennings, M. C.; Puddephatt, R. J. *Organometallics* **2006**, *25*, 1583.
(34) Iverson, C. N.; Carter, C. A. G.; Scollard, J. D.; Pribisko, M. A.; John, K. D.; Scott, B. L.; Baker, R. T.; Bercaw, J. E.; Labinger, J. A. *ACS Symp. Ser.* **2004**, *885*, 319.
(35) Scollard, J. D.; Day, M.; Labinger, J. A.; Bercaw, J. E. *Helv. Chim. Acta* **2001**, *84*, 3247.
(36) Reinartz, S.; White, P. S.; Brookhart, M.; Templeton, J. L. *Organometallics* **2000**, *19*, 3854.
(37) Rendina, L. M.; Puddephatt, R. J. *Chem. Rev.* **1997**, *97*, 1735.
(38) Smythe, N. A.; Grice, K. A.; Williams, B. S.; Goldberg, K. I. *Organometallics* **2009**, *28*, 277.
(39) Williams, B. S.; Holland, A. W.; Goldberg, K. I. *J. .Am. Chem. Soc.* **1999**, *121*, 252.
(40) Pawlikowski, A. V.; Getty, A. D.; Goldberg, K. I. *J. Am. Chem. Soc.* **2007**, *129*, 10382.
(41) Hill, G. S.; Yap, G. P. A.; Puddephatt, R. J. *Organometallics* **1999**, *18*, 1408.
(42) Hill, G. S.; Rendina, L. M.; Puddephatt, R. J. *J. Chem. Soc., Dalton Trans.* **1996**, 1809.
(43) Procelewska, J.; Zahl, A.; Liehr, G.; van Eldik, R.; Smythe, N. A.; Williams, B. S.; Goldberg, K. I. *Inorg. Chem.* **2005**, *44*, 7732.
(44) Heiberg, H.; Johansson, L.; Gropen, O.; Ryan, O. B.; Swang, O.; Tilset, M. *J. Am. Chem. Soc.* **2000**, *122*, 10831.
(45) Scheuermann, M. L.; Fekl, U.; Kaminsky, W.; Goldberg, K. I. *Organometallics* **2010**, *29*, 4749.
(46) Hux, J. E.; Puddephatt, R. J. *Inorg. Chim. Acta* **1985**, *100*, 1.
(47) Clegg, D. E.; Hall, J. R.; Swile, G. A. *J. Organomet. Chem.* **1972**, *38*, 403.
(48) West, N. M.; White, P. S.; Templeton, J. L.; Nixon, J. F. *Organometallics* **2009**, *28*, 1425.
(49) Clegg, D. E.; Swile, G. A.; Hall, J. R. *J. Organomet. Chem.* **1972**, *38*, 403.
(50) Kite, K.; Smith, J. A. S.; Wilkins, E. J. *J. Chem. Soc.* **1966**, 1744.
(51) Tolman, C. A. *Chem. Rev.* **1977**, *77*, 313.
(52) Pangborn, A. B.; Giardello, M. A.; Grubbs, R. H.; Rosen, R. K.; Timmers, F. J. *Organometallics* **1996**, *15*, 1518.
(53) Hill, G. S.; Irwin, M. J.; Levy, C. J.; Rendina, L. M.; Puddephatt, R. J. *Inorg. Synth.* **1998**, *32*, 149.
(54) Dochnahl, M.; Lohnwitz, K.; Pissarek, J. W.; Biyikal, M.; Schulz, S. R.; Schon, S.; Meyer, N.; Roesky, P. W.; Blechert, S. *Chem. Eur. J.* **2007**, *13*, 6654.
(55) Claramunt, R. M.; Sanz, D.; Perez-Torralba, M.; Pinilla, E.; Torres, M. R.; Elguero, J. *Eur. J. Org. Chem.* **2004**, 4452.